Since January 2020 Elsevier has created a COVID-19 resource centre with free information in English and Mandarin on the novel coronavirus COVID-19. The COVID-19 resource centre is hosted on Elsevier Connect, the company's public news and information website.

Distinguishing immune activation and inflammatory signatures of multisystem inflammatory syndrome in children (MIS-C) versus hemophagocytic lymphohistiocytosis (HLH)

Deepak Kumar, PhD,[a] Christina A. Rostad, MD,[b] Preeti Jaggi, MD,[b] D. Sofia Villacis Nunez, MD,[c] Chengyu Prince, BS,[a] Austin Lu, BS,[b] Laila Hussaini, MPH,[b] Thinh H. Nguyen, MD, PhD,[a] Sakshi Malik, PhD,[d,e] Lori A. Ponder, BS,[f] Sreekala P. V. Shenoy, MS,[c] Evan J. Anderson, MD,[b,g] Michael Briones, DO,[a] Ignacio Sanz, MD,[h,i] Sampath Prahalad, MD,[c,j] and Shanmuganathan Chandrakasan, MD[a] *Atlanta, Ga*

GRAPHICAL ABSTRACT

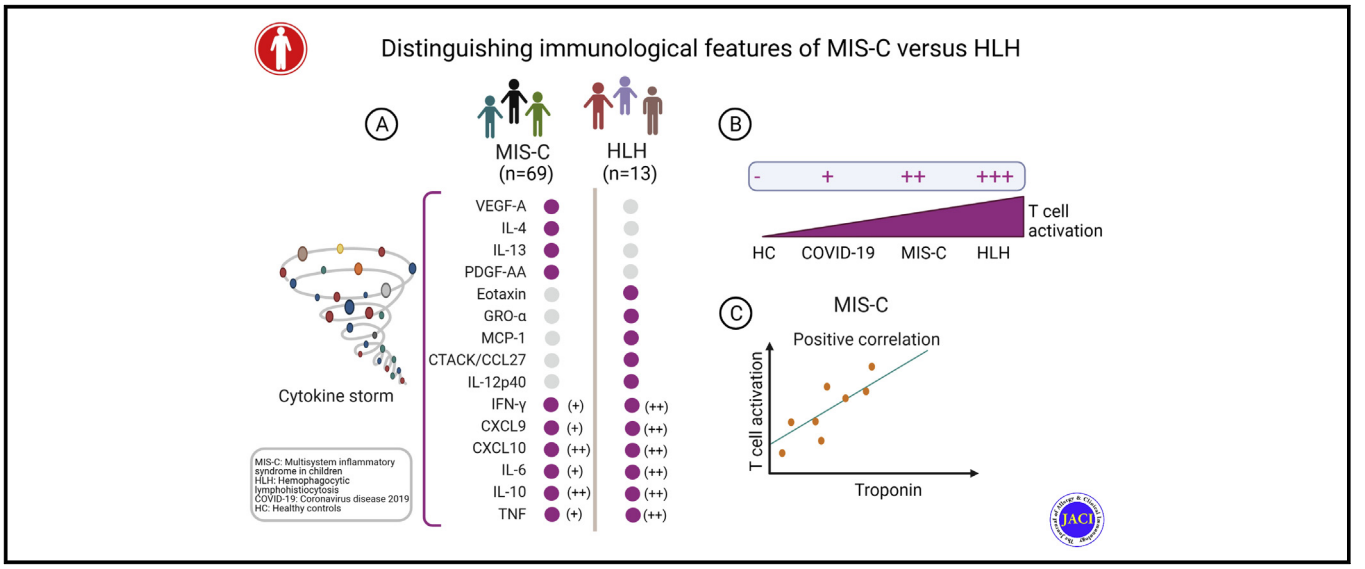

Background: Multisystem inflammatory syndrome in children (MIS-C) is a potentially life-threatening sequela of severe acute respiratory syndrome coronavirus 2 infection characterized by hyperinflammation and multiorgan dysfunction. Although hyperinflammation is a prominent manifestation of MIS-C, there is limited understanding of how the inflammatory state of

From [a]Aflac Cancer and Blood Disorders Center, Department of Pediatrics, [b]the Center for Childhood Infections and Vaccines, and [c]the Division of Pediatric Rheumatology, Department of Pediatrics, Children's Healthcare of Atlanta, Emory University School of Medicine, [d]Emory Vaccine Center and [e]the Department of Microbiology and Immunology, Emory University School of Medicine, [f]Children's Healthcare of Atlanta, [g]the Department of Medicine, and [h]the Division of Rheumatology, Department of Medicine, Emory University School of Medicine, [i]Lowance Center for Human Immunology, Emory University, and [j]the Department of Human Genetics, Emory University School of Medicine, Atlanta.

This work was supported by the National Heart, Lung, and Blood Institute (grant no. 1K08HL141635-01A1), Atlanta Pediatric Scholars Program K12 Scholar (grant nos. K12HD072245 and U54AI082973 to S.C.), and the National Institute of Allergy and Infectious Diseases 3U19AI110483-07S1 to I.S. (PI) and S.C. (Co-I) and S.P. (Co-I). S.P. is supported in part by the Marcus Foundation, Inc, Atlanta.

Disclosure of potential conflict of interest: S. Chandrakasan serves on the advisory committee for SOBI. S. Prahalad serves on a macrophage activation syndrome adjudication committee for Novartis Pharmaceuticals and is an Op-Med fellow for Doximity for 2021-2022. E. J. Anderson has consulted for Pfizer, Sanofi-Pasteur, Janssen, and Medscape, and his institution receives funds to conduct clinical research unrelated to this manuscript from MedImmune, Regeneron, PaxVax, Pfizer, GlaxoSmithKline (GSK), Merck, Sanofi-Pasteur, Janssen, and Micron. He also serves on a safety monitoring board for Kentucky BioProcessing, Inc, and Sanofi-Pasteur. His institution has also received funding from the National Institutes of Health to conduct clinical trials of Moderna and Janssen coronavirus disease 2019 vaccines. C. A. Rostad's institution has received funds to conduct clinical research unrelated to this manuscript from BioFire, Inc, GSK, MedImmune, Micron, Janssen, Merck, Moderna, Novavax, PaxVax, Pfizer, Regeneron, and Sanofi-Pasteur. The rest of the authors declare that they have no relevant conflicts of interest.

Received for publication October 18, 2021; revised February 18, 2022; accepted for publication February 23, 2022.

Available online March 15, 2022.

Corresponding author: Shanmuganathan Chandrakasan, MD, Immune Dysregulation and Immunohematology Program, Aflac Cancer and Blood Disorders Center, Children's Healthcare of Atlanta, Emory University School of Medicine, 2015 Uppergate Dr, ECC Rm 434A, Atlanta, GA 30322. E-mail: Shanmuganathan.chandrakasan@emory.edu.

0091-6749/$36.00

https://doi.org/10.1016/j.jaci.2022.02.028

MIS-C differs from that of well-characterized hyperinflammatory syndromes such as hemophagocytic lymphohistiocytosis (HLH).
Objectives: We sought to compare the qualitative and quantitative inflammatory profile differences between patients with MIS-C, coronavirus disease 2019, and HLH.
Methods: Clinical data abstraction from patient charts, T-cell immunophenotyping, and multiplex cytokine and chemokine profiling were performed for patients with MIS-C, patients with coronavirus disease 2019, and patients with HLH.
Results: We found that both patients with MIS-C and patients with HLH showed robust T-cell activation, markers of senescence, and exhaustion along with elevated T_H1 and proinflammatory cytokines such as IFN-γ, C-X-C motif chemokine ligand 9, and C-X-C motif chemokine ligand 10. In comparison, the amplitude of T-cell activation and the levels of cytokines/chemokines were higher in patients with HLH when compared with patients with MIS-C. Distinguishing inflammatory features of MIS-C included elevation in T_H2 inflammatory cytokines such as IL-4 and IL-13 and cytokine mediators of angiogenesis, vascular injury, and tissue repair such as vascular endothelial growth factor A and platelet-derived growth factor. Immune activation and hypercytokinemia in MIS-C resolved at follow-up. In addition, when these immune parameters were correlated with clinical parameters, $CD8^+$ T-cell activation correlated with cardiac dysfunction parameters such as B-type natriuretic peptide and troponin and inversely correlated with platelet count.
Conclusions: Overall, this study characterizes unique and overlapping immunologic features that help to define the hyperinflammation associated with MIS-C versus HLH. (J Allergy Clin Immunol 2022;149:1592-606.)

Key words: *MIS-C, COVID-19, HLH, T-cell activation, hyperinflammation, cardiac dysfunction*

Abbreviations used

BNP:	B-type natriuretic peptide
COVID-19:	Coronavirus disease 2019
CRP:	C-reactive protein
CXCL9:	C-X-C motif chemokine ligand 9
CXCL10:	C-X-C motif chemokine ligand 10
EM:	Effector memory
HC:	Healthy control
HLH:	Hemophagocytic lymphohistiocytosis
KD:	Kawasaki disease
MIS-C:	Multisystem inflammatory syndrome in children
PDGF:	Platelet-derived growth factor
ROC:	Receiver-operating characteristic
sIL-2R:	Soluble IL-2 receptor
TMA:	Thrombotic microangiopathy
VEGF-A:	Vascular endothelial growth factor A

Coronavirus disease 2019 (COVID-19) is less likely to result in hospitalization and death in children as compared with adults and older individuals[1,2]; however, children can develop a life-threating complication following exposure to severe acute respiratory syndrome coronavirus 2 (SARS-COV-2) known as multisystem inflammatory syndrome in children (MIS-C).[3,4] MIS-C is characterized by a prominent cardiac dysfunction with elevation of both B-type natriuretic peptide (BNP) and troponin. In addition to the heart, MIS-C affects multiple organs including the gastrointestinal tract, lungs, kidneys, brain, skin, or eyes.[5,6] Because of prominent cardiac complications and hemodynamic instability, initial studies focused on differentiating MIS-C from Kawasaki disease (KD) or toxic shock syndrome. Systematic studies identified unique cardiac phenotypes in MIS-C characterized by more global cardiac dysfunction and myocarditis than in KD.[7,8] Furthermore, KD is more commonly seen in children younger than 5 years,[9] whereas MIS-C is observed more frequently after age 5 years.[1] Further studies focused on immunobiology comparing the pathophysiology of MIS-C and KD revealed that MIS-C differs from KD. Lower frequency of T follicular helper cells was found in patients with MIS-C[10] and more IL-17A–mediated inflammation in KD.[11]

Another pathognomonic manifestation of MIS-C is the systemic hyperinflammation.[12] Some features such as hyperferritinemia, cytopenia, and elevated liver enzymes are reminiscent of hemophagocytic lymphohistiocytosis (HLH).[12-14] In addition, management with high-dose steroids and biologics overlaps with the management of HLH.[15,16] Thus far, limited data differentiating the immune signatures of MIS-C and HLH are available to provide insights into pathogenesis and ultimately patient management. Also, quantitative comparison of the T-cell activation state in MIS-C versus HLH has not been previously evaluated.

Using T-cell immunophenotyping and multiplex cytokine and chemokine profiling, we evaluated the immune signatures of children hospitalized for MIS-C and COVID-19 and compared them with those of children with HLH and healthy controls (HCs). We also evaluated how inflammatory markers correlated with cardiac dysfunction. Our findings could help understand the unique inflammatory milieu that contributes to the clinical manifestations observed in MIS-C.

METHODS

Human subjects

Children with MIS-C and COVID-19 were enrolled between April 2020 and April 2021 at Children's Healthcare of Atlanta. Patients with MIS-C were enrolled on the basis of case definition as described by the Centers for Disease Control and Prevention.[17] Patients with HLH and age-matched HCs were included as a comparison cohort for MIS-C and COVID-19. Patients with HLH had mainly primary HLH, or EBV infection–associated HLH, and all of them fulfilled HLH-2004 diagnostic criteria.[13] All patients were enrolled following informed consent, with approval by the Emory University Institutional Review Board.

Flow cytometry and analysis

PBMCs were used for immunophenotyping. Antibody information is provided in this article's Online Repository at www.jacionline.org. Flow cytometry data were acquired on BD FACSymphony A5 (BD Biosciences, Franklin Lakes, NJ) and analyzed using FlowJo software v10 (BD, Ashland, Ore). T-cell activation was defined by coexpression of $HLA\text{-}DR^+$ and $CD38^+$ on effector memory (EM) $CD4^+$ and $CD8^+$ T cells.[18-20] Coexpression of $PD\text{-}1^+$ and $Tim3^+$ on EM $CD4^+$ and $CD8^+$ T cells was defined as a marker for exhaustion.[21] T-cell senescence was assessed by expression of $CD57^+$ on the EM population of $CD4^+$ and $CD8^+$ T cells.[22-25] Definitions of T-cell populations analyzed in this study are presented in Table E1 in this article's Online Repository at www.jacionline.org.

TABLE I. Description of demographic characteristics and clinical parameters of patient cohorts

Parameters	n	MIS-C	n	COVID-19	*P* value
Demographic data					
Age (y), median (range)	69	11 (2-19)	24	11.5 (2-17)	.13
Sex (male:female)	69	50:19	24	9:15	.003
Clinical data					
WBC* (cells/μL), median (range)	69	14,340 (4,140-47,240)	21	12140 (5,260-65,720)	.083
ANC* (cells/μL), median (range)	69	12,040 (2,620-34,020)	21	7,200 (2,410-22,450)	.009
ALC† (cells/μL), median (range)	69	648 (140-2,706)	20	996 (200-6,776)	.024
Platelet counts† ($\times 10^3$ cells/μL), median (range)	69	140 (18-726)	22	226 (19-447)	<.0001
Creatinine* (mg/dL), median (range)	69	0.66 (0.32-7.49)	20	0.59 (0.25-1.11)	.1
ALT* (U/L), median (range)	69	47 (12-2,109)	19	47 (16-205)	.98
BNP* (pg/mL), median (range)	69	690.1 (19.8-6,995)	15	24.5 (10-852)	<.0001
Troponin* (ng/mL), median (range)	69	0.15 (0.015-13.8)	15	0.02 (0.015-1.92)	.002
Ferritin* (ng/mL), median (range)	67	594.7 (89.73-4,744)	16	137.66 (9.1-982.39)	<.0001
sIL-2R (U/mL), median (range)	48	4792 (525.6-20,816)	21	1091 (328.5-6,106)	<.0001
CRP* (mg/dL), median (range)	69	15.7 (3.9-43.7)	18	8.3 (0.3-23.9)	<.0001
ICU admission	69	49	24	14	.31
Low flow O_2	69	31	24	12	.81
High flow O_2	69	24	24	8	>.9999

Values in parentheses represent observed range of each parameter.
ALC, Absolute lymphocyte count; *ALT*, alanine transaminase; *ANC*, absolute neutrophil count; *ICU*, intensive care unit; *WBC*, white blood cell count.
*Maximum values recorded.
†Minimum values recorded.

Plasma cytokine/chemokine profiling

Cytokine/chemokine profiling of plasma samples from patients with COVID-19 (n = 10), HLH (n = 8), MIS-C (n = 19), and MIS-C follow-up (n =10) and from HCs (n = 19) was performed on a luminex platform. The plasma samples for cytokine/chemokine profiling were chosen randomly from a cohort of 69 patients with MIS-C and 24 patients with COVID-19. A list of these analytes is provided in Table E2 in this article's Online Repository at www.jacionline.org. Soluble IL-2 receptor (sIL-2R) and ferritin levels were done in clinical lab as standard of care. Plasma levels of sCD163 were measured using human CD163 ELISA kit (Abcam, ab274394; Boston, Mass) as per manufacturer's instructions.

Statistics

Cytokine/chemokine data were represented as dot plots showing all the data points using Graphpad Prism version 9 (GraphPad Software, San Diego, Calif). One-way ANOVA with multiple comparison test was used for calculating significant differences between groups. Frequencies of immune parameters were represented with median and interquartile range. Fisher exact test was used to compute significance for categorical data. We applied a principal-component analysis on all the cytokines showing differences among patient groups based on principal-component 1 and principal-component 2 and created using Factoextra R package. Heatmap of all the reported cytokines was generated in pheatmap R package. Spearman correlation was used to find the correlation between clinical and flow-based parameters; correlation coefficients and *P* values were reported. Correlation matrix was made in "corrplot" package in R.

RESULTS

Cohort description and clinical characteristics

We enrolled 69 patients with MIS-C (age, 2-19 years; median, 11 years), 24 patients hospitalized with COVID-19 but without MIS-C (age, 2-17 years; median, 11.5 years), 13 patients with HLH (age, 1 day-19.3 years; median, 1.2 years), and 22 HCs (age, 8-25 years; median, 17 years).

The demographic characteristics, clinical parameters, and standard of care laboratory tests for patients with MIS-C, COVID-19, and HLH are detailed in Table I and in Table E3 in this article's Online Repository at www.jacionline.org. A follow-up immune evaluation was performed for 31 patients with MIS-C, median follow-up of 2 months postdiagnosis of MIS-C (range, 1-7 months) (see Fig E1 in this article's Online Repository at www.jacionline.org).

Seventy-one percent of patients with MIS-C required intensive care unit care, whereas 58.3% of patients with COVID-19 were admitted to intensive care unit. Most patients with MIS-C were treated with steroids and intravenous immunoglobulin (see Fig E2 in this article's Online Repository at www.jacionline.org). In our cohort, children with MIS-C had higher ferritin, C-reactive protein (CRP), neutrophil count, and thrombocytopenia compared with those with COVID-19 (Table I), consistent with the previously published reports.[6,11,26,27]

Inflammatory milieu reveals differences and similarities between MIS-C and HLH

To investigate how qualitatively the inflammatory response of patients with MIS-C differs from that of patients with HLH in plasma, we performed multiplex cytokine/chemokine profiling of 66 analytes in MIS-C (n = 19), MIS-C follow-up (n = 10), COVID-19 (n = 10), HLH (n = 8), and HCs (n = 19) (Fig 1, *A*). Principal-component analysis of all these cytokines showed that both patients with HLH and patients with MIS-C formed distinct clusters in comparison with patients with COVID-19, HCs, and follow-up MIS-C patients (Fig 1, *B*).

We observed a cluster of 17 cytokines, that is, IFN-γ, C-X-C motif chemokine ligand 9 (CXCL9), C-X-C motif chemokine ligand 10 (CXCL10), TNF, IL-6, IL-8, IL-10, IL-15, IL-18, IL-27, IL-1α, IL-1RA, CXCL13, FLT-3L, M-CSF, MIP-1β, and MCP-2, that were significantly elevated in both patients with MIS-C and patients with HLH. A decreased level of macrophage-derived chemokine or CCL22 was observed in patients with HLH and patients with MIS-C. Of these cytokines, concentrations of CXCL9, IL-6, IL-8, IL-18, and M-CSF were

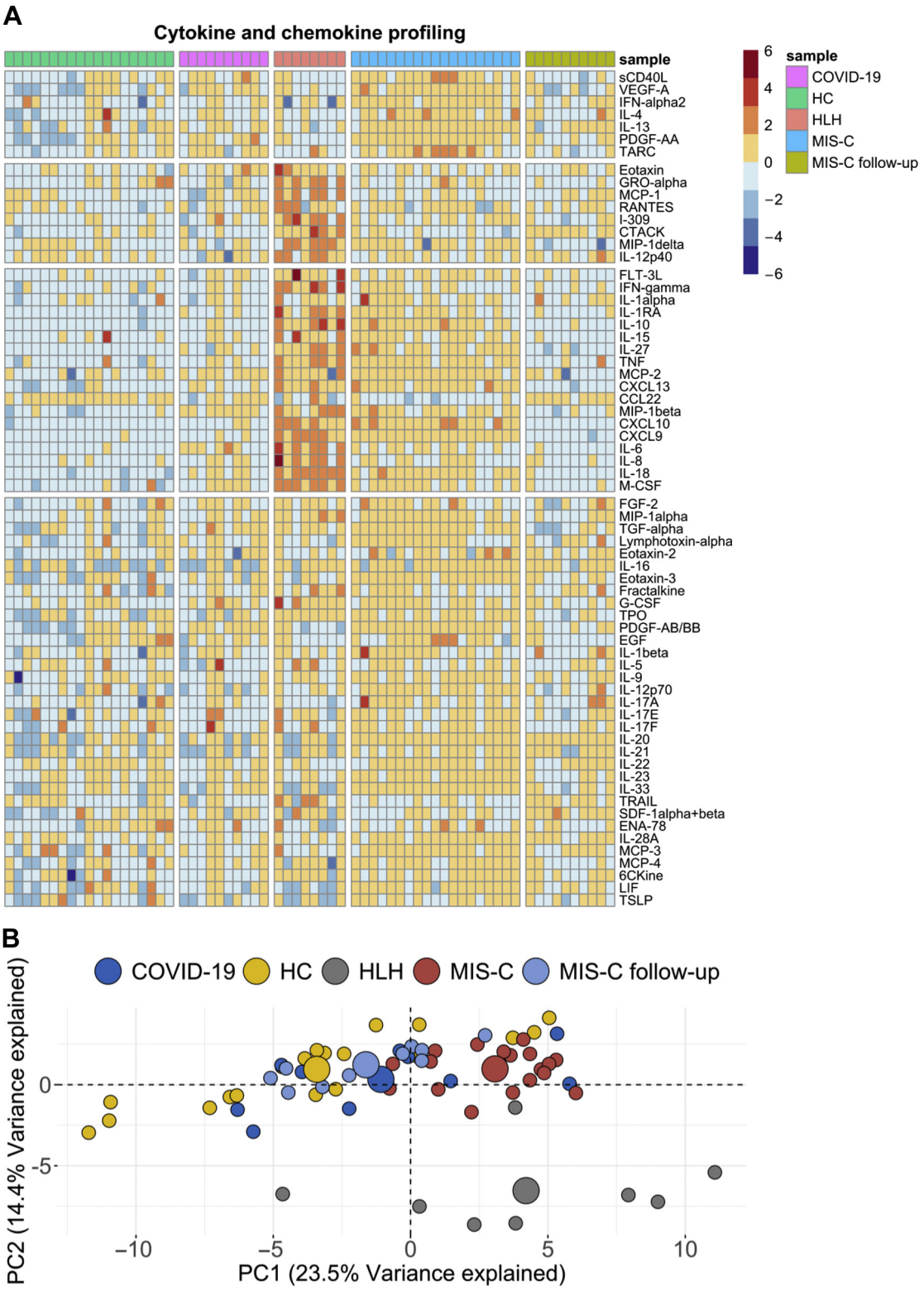

FIG 1. MIS-C and HLH display both unique and shared inflammatory signature. **A,** Heat map showing expression of cytokines and chemokines in HCs (n = 19), COVID-19 (n = 10), HLH (n = 8), MIS-C (n = 19), and MIS-C follow-up (n = 10) samples. **B,** Multidimensional cytokine/chemokine data were represented as 2-dimensional PCA space showing clusters for HCs, COVID-19, MIS-C, HLH, and MIS-C follow-up samples. Individuals are shown by small-size colored circles, whereas overall group is shown by large-size colored circles. *PC*, Principal component; *PCA*, principal-component analysis.

higher in patients with HLH as compared with patients with MIS-C.

Next, we also looked at the unique cytokine signature in patients with MIS-C. Importantly, significant elevation in vascular endothelial growth factor A (VEGF-A), sCD40L, IFN-α2, IL-4, IL-13, platelet-derived growth factor (PDGF)-AA, and TARC was found only in patients with MIS-C but not in patients with HLH. However, eotaxin, GRO-α, MCP-1, RANTES, I309, cutaneous T-cell–attracting chemokine, MIP-1δ, and IL-12p40 were significantly increased in patients with HLH but not in patients with MIS-C. Cytokines such as MIP-1α, TGF-α, lymphotoxin-alpha, eotaxin-2, eotraxin-3, and IL-16 were significantly elevated in patients with MIS-C as compared with controls, but we did not find a significant difference between patients with HLH and patients with MIS-C. Similarly, fractalkine, G-CSF, and TPO were significantly elevated in patients with HLH as compared with HCs but did not show differences with respect to patients with MIS-C. In children with COVID-19, a limited number of cytokines such as IL-1RA, IL-6, PDGF-AA, MIP-1β, and MCP2 were significantly elevated.

Next, we sought to investigate the cytokine families that were differentially regulated in these cohorts. In general, patients with MIS-C showed prominent elevations in different cytokine families (Fig 2, *A-F*). Cytokines and chemokines related to T-cell activation such as IFN-γ, IL-6, TNF, CXCL9, and CXCL10 were significantly elevated in both MIS-C and HLH groups. However, the amplitude of these cytokines was higher in patients with HLH when compared with the amplitude in patients with MIS-C (Fig 2, *A*). Interestingly, cytokine mediators responsible for angiogenesis, vascular injury, and tissue repair such as VEGF-A ($P < .0001$), PDGF-AA ($P < .05$), PDGF-AA/AB ($P = .07$), and FGF-2 ($P = .06$) were elevated in patients with MIS-C when compared with HCs but not in patients with HLH (Fig 2, *E*). Increased levels of these cytokines were also observed in some patients with COVID-19, although overall we did not find significance between COVID-19 and HC cohorts except for PDGF-AA ($P = .04$). T_H2 inflammatory cytokines (ie, IL-4, IL-13) were significantly elevated in patients with MIS-C but not in patients with HLH. All the remaining cytokines are shown in Fig E3 in this article's Online Repository at www.jacionline.org. As previously reported, we also evaluated whether the values of TNF and IL-10 in combination can differentiate between MIS-C and COVID-19 in our cohorts.[28] We found similar observations where the sum of the plasma levels of TNF and IL-10 was significantly elevated in patients with MIS-C versus patients with COVID-19 (Fig E3 extended).

Overall, these data demonstrate that patients with MIS-C and patients with HLH have some overlap in the inflammatory milieu; however, the amplitude of the inflammation is much higher in patients with HLH. In addition, differential expression of certain inflammatory cytokines and chemokines in patients with MIS-C suggests unique inflammatory pathways that are active in patients with MIS-C but not in patients with HLH.

T-cell activation is higher in MIS-C and overlaps with HLH

Increased T-cell activation has been reported in both pediatric COVID-19 and MIS-C.[29-31] A profound elevation of IFN-γ and its induced chemokines, that is, CXCL9 and CXCL10[32-34] and other inflammatory markers such as IL-6 and TNF, in patients with HLH when compared with patients with MIS-C suggests higher T-cell activation in HLH in comparison to MIS-C. To further strengthen these observations and to investigate how T-cell activation in MIS-C and COVID-19 compares with that of HLH, we assessed the expression of activation markers on $CD4^+$ and $CD8^+$ T-cell subsets. The gating strategy for these analyses is shown in Fig E4 in this article's Online Repository at www.jacionline.org. We first evaluated HLA-DR^+ $CD38^+$ expression in the EM compartment of $CD4^+$ and $CD8^+$ T cells. $CD8^+$ EM T-cell activation was noted in both patients with COVID-19 and patients with MIS-C. In COVID-19, the T-cell activation was modest (5-fold; $P = .0022$), whereas MIS-C showed higher activation (13-fold; $P < .0001$) when compared with the median for HCs. Quantitatively, the amplitude of $CD8^+$ EM T-cell activation in patients with HLH was 2-fold greater than that in patients with MIS-C. Although $CD8^+$ EM T-cell activation was significantly higher in patients with HLH than in patients with MIS-C, we observed that a subset of patients with MIS-C had similar $CD8^+$ EM T-cell activation as of patients with HLH (Fig 3, *A* and *C*). Similarly, although the $CD4^+$ EM T compartment was activated in both patients with MIS-C and patients with HLH (Fig 3, *B* and *D*), $CD4^+$ EM T-cell activation was 6 times higher in patients with HLH than in patients with MIS-C. Using receiver-operating characteristic (ROC) statistics, we calculated the optimal threshold value for $CD8^+$ EM T-cell activation that can differentiate patients with MIS-C from HCs, patients with COVID-19, and patients with HLH with high sensitivity and specificity (see Fig E5, *A-C*, in this article's Online Repository at www.jacionline.org). We observed that $CD8^+$ EM T-cell activation more than 79.9% can differentiate patients with HLH from patients with MIS-C with high area under the ROC curve (0.99) along with high sensitivity (100%) and specificity (98.6%). Similarly, cutoff of $CD8^+$ EM T-cell activation more than 15.9% (area under the ROC curve, 0.98; sensitivity, 89.9%; specificity, 95.5%) and more than 27.4% (area under the ROC curve, 0.79; sensitivity, 72.5%; specificity, 75%) could help differentiate MIS-C from HC and COVID-19, respectively. To provide a more global picture of T-cell activation, we also evaluated HLA-DR^+ $CD38^+$ expression on central memory and TEMRA populations of $CD4^+$ and $CD8^+$ T cells and also on total $CD4^+$ and $CD8^+$ cells. A similar trend of activation was observed as seen previously in the EM compartment (see Fig E6 in this article's Online Repository at www.jacionline.org).

T-cell activation measured by the expression of HLA-DR^+ $PD\text{-}1^+$ on the EM compartment of $CD4^+$ and $CD8^+$ T cells also showed similar trends noted with HLA-DR^+ and $CD38^+$ expression. The expression of HLA-DR^+ $PD\text{-}1^+$ was significantly elevated in both $CD4^+$ and $CD8^+$ T cells in patients with MIS-C as well as patients with HLH; however, the expression of HLA-DR^+ $PD\text{-}1^+$ was much higher in patients with HLH as compared with patients with MIS-C (Fig 3, *E* and *F*). Because we observed increased activation in $CD8^+$ T EM compartment in MIS-C cohorts, we aimed to further evaluate whether increased activation in CD8 EM compartment resulted in relative expansion of $CD8^+$ EM compartment. Therefore, we calculated the ratio of the frequencies of EM and naive compartments. Interestingly, we found a relative expansion of the EM compartment in patients with HLH but not in patients with MIS-C (see Fig E7, *A*, in this article's Online Repository at www.jacionline.org). The $CD4^+$/$CD8^+$ ratio was similar between patients with MIS-C and patients with HLH. When compared with patients with MIS-C, patients

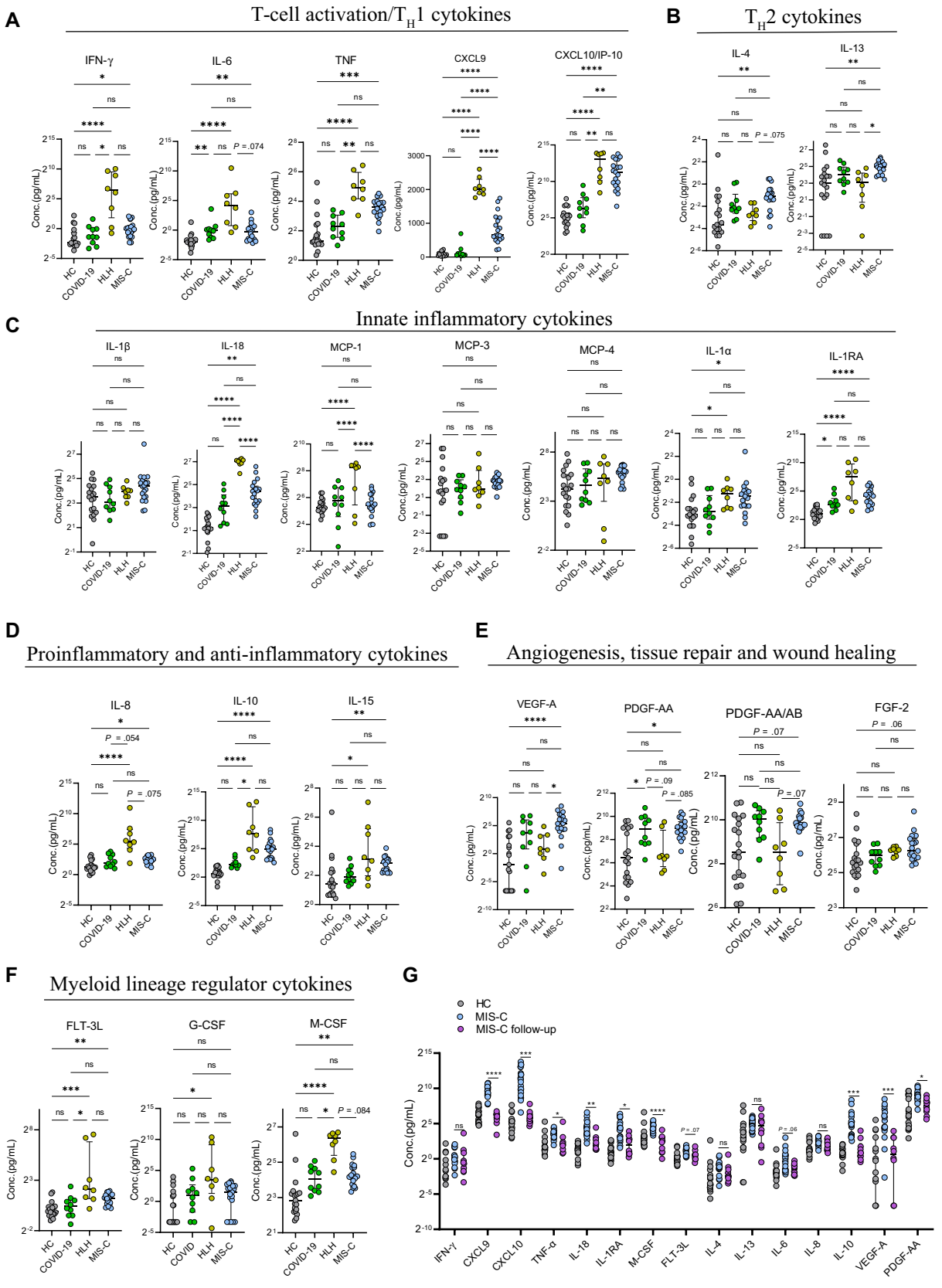

FIG 2. A-G, Cytokine families showing differences in patients with MIS-C and patients with HLH. Plasma levels of important cytokines belonging to multiple cytokine families were represented by dot plots in HCs (n = 19), COVID-19 (n = 10), HLH (n = 8), MIS-C (n = 19), and MIS-C follow-up (n = 10) samples. *Conc.*, Concentration; *ns*, not significant. Kruskal-Wallis 1-way ANOVA followed by Dunn's multiple comparison test for nonnormally distributed samples and ordinary 1-way ANOVA followed by Tukey's multiple comparison test for normally distributed samples were used for statistical comparison. **P* < .05, ***P* < .01, ****P* < .001; *****P* < .0001.

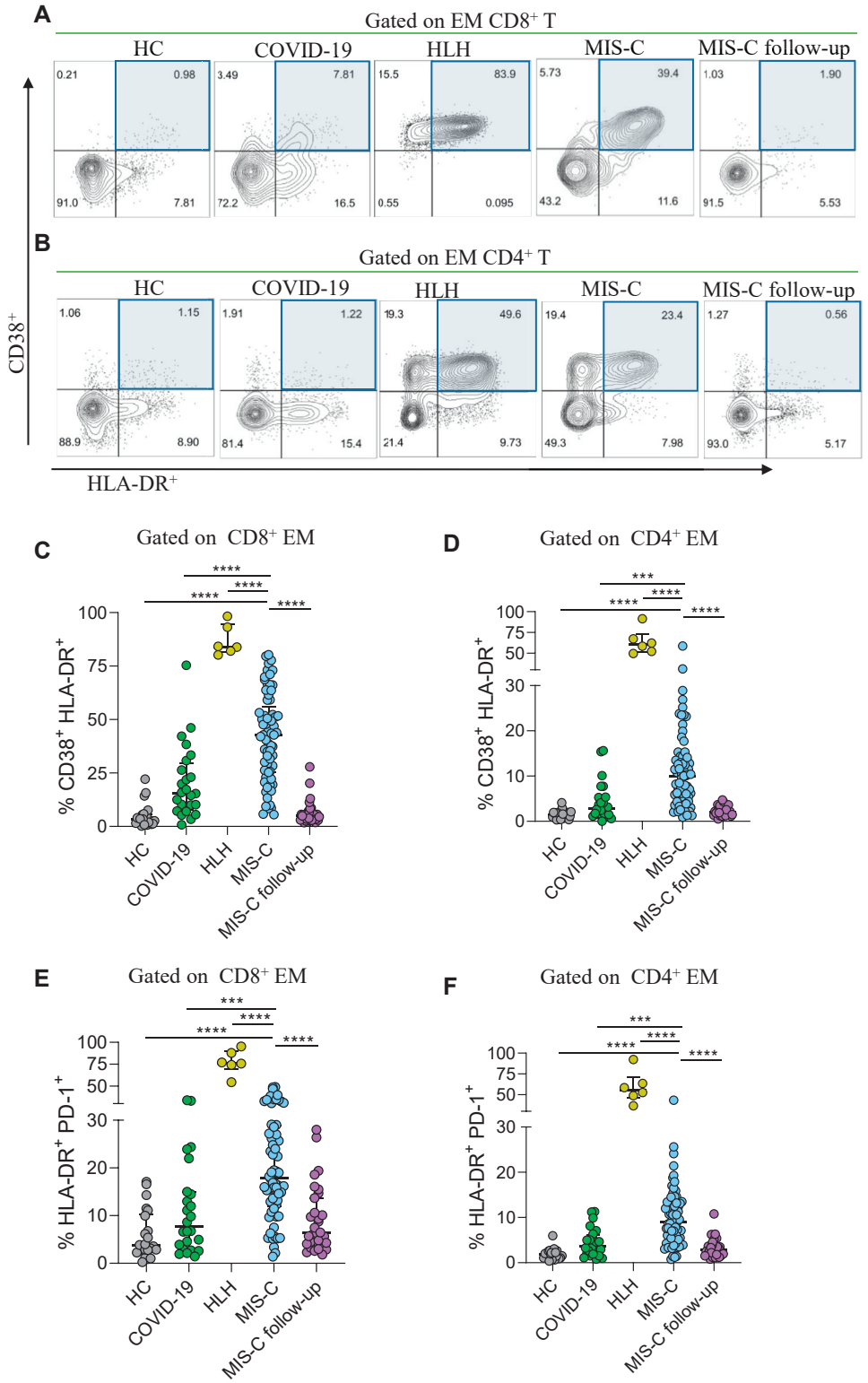

FIG 3. MIS-C and HLH are marked by increase in activation of $CD8^+$ and $CD4^+$ EM T cells. **A** and **B,** Representative FACS plots showing surface expression of HLA-DR^+ $CD38^+$ markers on the EM compartment of $CD8^+$ and $CD4^+$ T cells in HCs and COVID-19, HLH, MIS-C, and MIS-C follow-up patients. **C-F,** Percentage of HLA-DR^+ $CD38^+$ and HLA-DR^+PD-1^+ expression in HCs (n = 22) and COVID-19 (n = 24), HLH (n = 6), MIS-C (n = 69), and MIS-C follow-up (n = 31) patients in $CD8^+$ and $CD4^+$ EM compartments. *FACS*, Fluorescence-activated cell sorting; *ns*, not significant. Data represent median with interquartile range values for each group. Kruskal-Wallis 1-way ANOVA followed by Dunn's multiple comparison test for non-normally distributed samples and ordinary 1-way ANOVA followed by Tukey's multiple comparison test for normally distributed samples were used for statistical comparison. ***$P < .001$; ****$P < .0001$.

with COVID-19 had overall higher $CD4^+/CD8^+$ ratio, although nonsignificant (Fig E7, *B*). Next, we also evaluated $CD4^+$ and $CD8^+$ TEMRA populations. Although TEMRA populations were similar among different patient cohorts, we found an increase of this subset in MIS-C follow-up patients when compared with onset MIS-C patients (Fig E7, *C* and *D*).

Patients with MIS-C are marked by high surface markers of T-cell exhaustion and senescence

Patients with MIS-C have been reported to have prolonged presence of severe acute respiratory syndrome coronavirus 2 in the gastrointestinal tract[35]; thus, we hypothesized that chronic antigenic exposure in MIS-C and associated T-cell activation could potentially lead to a postactivation exhaustion state of T cells and show features of proliferation-induced senescence. To test these hypotheses, we evaluated the expression of T-cell exhaustion and senescence surface markers in $CD4^+$ and $CD8^+$ EM T cells for these patient cohorts. T-cell exhaustion was evaluated by coexpression of PD-1^+ and Tim3^+ on EM $CD4^+$ and $CD8^+$ T cells. Significant increase in T-cell exhaustion markers was observed in both patients with MIS-C and patients with HLH in both $CD4^+$ and $CD8^+$ EM T cells; however, the frequency of cells expressing exhaustion markers was much higher in patients with HLH when compared with patients with MIS-C (Fig E7, *E* and *F*). We also observed a modest increase in exhaustion markers in patients with COVID-19 when compared with HCs in both $CD4^+$ and $CD8^+$ T EM compartments. Also, patients with MIS-C displayed significantly higher $CD57^+$ expression on $CD8^+$ EM cells (Fig E7, *G*). Interestingly, we did not find any difference in $CD57^+$ expression for COVID-19 and HLH cohorts when compared with HCs. Similarly, we found a significant increase in the expression of $CD57^+$ on $CD4^+$ EM T cells in patients with MIS-C (Fig E7, *H*). Although patients with COVID-19 did not show any difference, patients with HLH showed a marked increase in $CD57^+$ expression when compared with HCs. These phenotypic markers of exhaustion and senescence on T cells reassuringly return to HCs range at follow-up in patients with MIS-C.

Clinical parameters of MIS-C and COVID-19 overlap with HLH

To understand where patients with MIS-C and patients with COVID-19 fall into the clinical spectrum of HLH, we evaluated patients with MIS-C and patients with COVID-19 based on clinical laboratory parameters defined in the 2004 HLH criteria.[13] We compared some important clinical and laboratory features such as cytopenias, ferritin, fibrinogen, and sIL-2R in patients with MIS-C and patients with COVID-19. About 83.3% and 33.3% of patients with MIS-C and patients with COVID-19, respectively, had sIL-2R levels greater than or equal to 2400 U/mL; 61.2% and 18.8% of patients with MIS-C and patients with COVID-19, respectively, were noted to have ferritin levels greater than or equal to 500 ng/mL. In patients with MIS-C, 16.7% had platelets less than 100×10^9/L, 3.4% had absolute neutrophil count less than 1.0×10^9/L, 3.3% had hemoglobin less than 90 g/L, and 1.8% had fibrinogen less than or equal to 1.5 g/L. However, none of the patients with COVID-19 had low platelets, absolute neutrophil count, hemoglobin, and fibrinogen as per 2004 HLH criteria (see Table E4 in this article's Online Repository at www.jacionline.org). Recent publications have evaluated overlap of MIS-C and COVID-19 with HLH, and our cohort validates some of these findings.[36] Although we compared important parameters of HLH 2004 criteria, a formal application of these criteria was not possible because all the clinical and lab parameters needed for evaluation were not obtained in all patients. However, individual laboratory parameters that were consistently available for these patients were assessed. A direct comparison of standard parameters of HLH such as ferritin, sIL-2R, and sCD163 revealed that patients with HLH had significantly higher plasma levels of ferritin, sIL-2R, and sCD163 when compared with patients with MIS-C, whereas patients with COVID-19 had lower levels of ferritin, sIL-2R, and sCD163 when compared with patients with MIS-C (Fig 4, *A-C*). These findings validate the T-cell activation and inflammatory signature as seen in our previous observations.

Neutrophil to lymphocyte ratio has been proposed as a distinguishing parameter in MIS-C and COVID-19 illness.[26,37] As reported previously, neutrophil to lymphocyte ratio was higher in patients with MIS-C when compared with patients with COVID-19, with a trend toward significance (median, 8.2 vs 3.8; $P = .06$). However, this ratio was significantly lower in patients with HLH compared with patients with COVID-19 (median, 0.34 vs 3.8; $P = .005$) and patients with MIS-C (median, 0.34 vs 8.2; $P < .0001$) (Fig 4, *D*). In addition, to determine whether the neutrophil counts differ with respect to T-cell activation in these patient cohorts, we assessed the ratio of ANC with $CD8^+$ and $CD4^+$ EM T-cell activation. We observed that these ratios could easily distinguish these clinical entities because these were higher in patients with COVID-19 when compared with patients with MIS-C ($P = .08$) and patients with HLH ($P < .001$), whereas patients with HLH had significantly lower ratios when compared with patients with MIS-C and patients with COVID-19 (Fig 4, *E* and *F*).

Inflammatory markers resolve at follow-up in patients with MIS-C

Although previous studies describing immunophenotypic differences in MIS-C have only focused on the acute disease state at onset, follow-up studies are limited.[26] In our study, we assessed T-cell–based immune markers as well as cytokine/chemokine profile during follow-up. Immune evaluation of patients with MIS-C at follow-up revealed a significant decrease in both $CD4^+$ and $CD8^+$ EM T-cell activation with return to HCs (Fig 3, *C-F*; see Fig E8 in this article's Online Repository at www.jacionline.org). In addition, we observed a decrease in T-cell exhaustion as well as senescence markers at follow-up in both CD4 and CD8 EM subsets (Fig E7, *E-H*, and Fig E8). In a subset of patients with MIS-C, we also assessed the levels of cytokines and chemokines at follow-up. Almost all of the elevated cytokines had resolved to normal levels in patients with MIS-C (Fig 2, *G*). We also assessed some clinical inflammatory markers such as ferritin and CRP at hospital admission and after 7 days of follow-up in some patients with MIS-C for whom longitudinal data were available and found a significant decrease in their levels on follow-up, suggesting rapid response of systemic inflammation with treatment (Fig E8, *F*).

T-cell activation correlates with cardiac inflammatory markers in patients with MIS-C

MIS-C and severe COVID-19 have been found associated with rise in acute myocardial markers such as BNP and

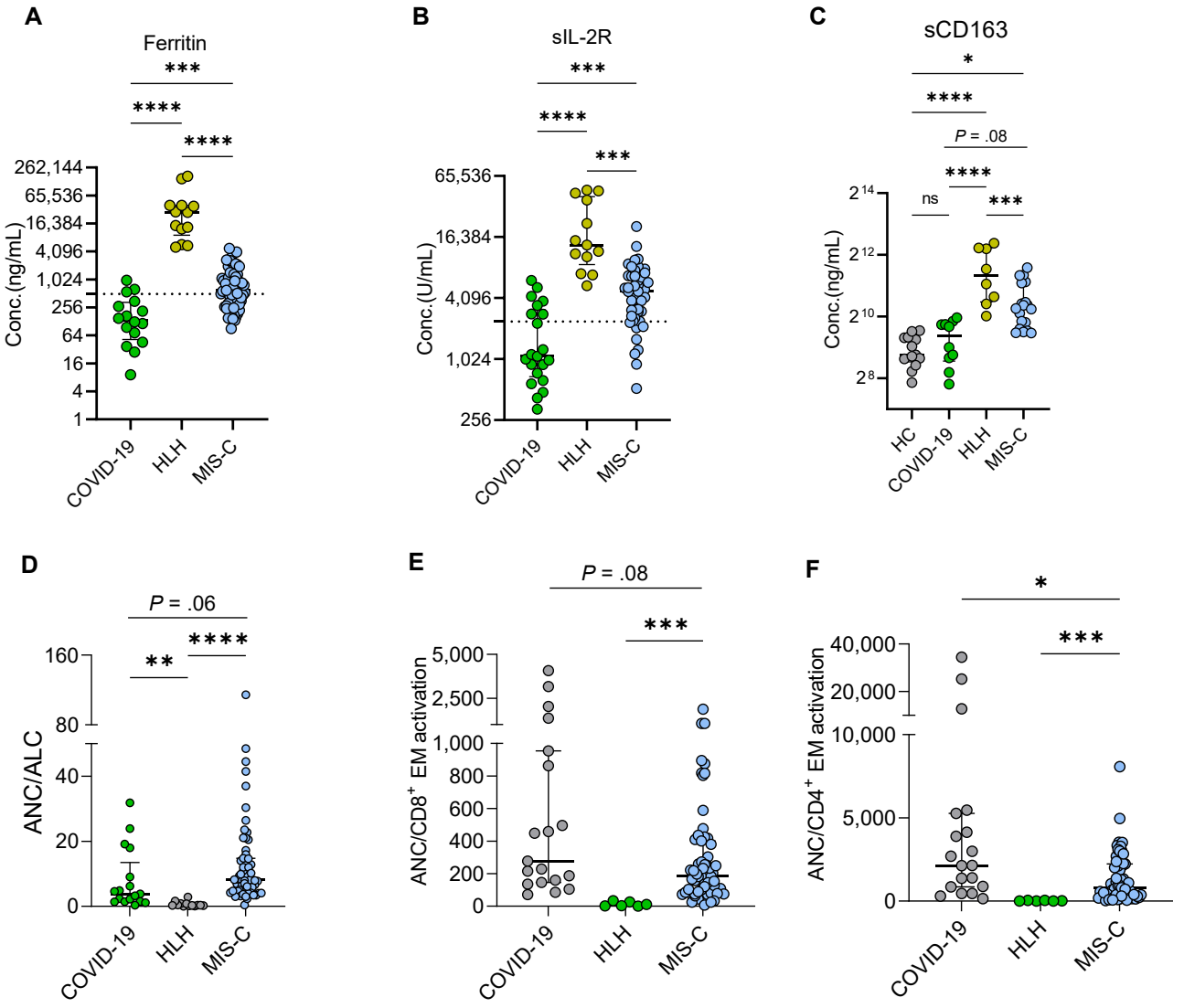

FIG 4. Comparison of different laboratory parameters in patients with COVID-19, HLH, and MIS-C. Dot plots showing the plasma levels of ferritin (**A**), sIL-2R (**B**), and sCD163 (**C**) in different patient cohorts. Dotted lines represent ferritin cutoff levels of 500 ng/mL and sIL-2R cutoff levels of 2400 U/mL. **D,** Plots showing NLR in different patient cohorts. **E** and **F,** Plots showing ratio of ANC with $CD8^+$ and $CD4^+$ EM T-cell activation. *ALC,* Absolute lymphocyte count; *ANC,* absolute neutrophil count; *Conc.,* concentration; *NLR,* neutrophil to lymphocyte ratio.

troponin.[26,38-40] To investigate whether T-cell activation correlates with the cardiac inflammatory markers and disease severity in COVID-19 and MIS-C, we first compared the BNP and troponin levels in patients with COVID-19 and patients with MIS-C. In our cohort, we found that both BNP and troponin are significantly higher in patients with MIS-C as compared with patients with COVID-19, validating the high occurrence of cardiac dysfunction and cardiac injury in patients with MIS-C (see Fig E9, *A* and *B*, in this article's Online Repository at www.jacionline.org). We next checked whether there is an association of cardiac dysfunction markers with T-cell activation in patients with MIS-C and patients with COVID-19. We found a correlation of troponin levels with $CD8^+$ and $CD4^+$ EM T-cell activation (Fig 5, *A* and *B*). Similarly, BNP levels correlated with $CD8^+$ EM T-cell activation as well as $CD4^+$ EM T-cell activation (Fig 5, *C* and *D*). We found that patients with T-cell activation greater than the threshold value of more than 15.9% $CD8^+$ EM activation (threshold determined on the basis of ROC between MIS-C and HCs) have significantly high BNP and troponin levels as compared with patients with T-cell activation lower than the cutoffs values (Fig E9, *C* and *D*). Next, we chose cutoff values for BNP (200 pg/mL; 2 times the upper limit of normal) and troponin (0.09 ng/mL; 2 times the upper limit of normal) for calculating the odds ratio of finding high BNP or troponin in patients with high $CD8^+$ EM T-cell activation. Our data showed that patients having higher $CD8^+$ EM T-cell activation (>15.9%) were 9.1 times (95% CI, 2.7-30.1) more likely to have elevated BNP levels (>200 pg/mL) than patients with low T-cell activation. Similarly, patients with high $CD8^+$ EM T-cell activation were 6.2 (95% CI, 1.8-21.3) times more likely to have high troponin

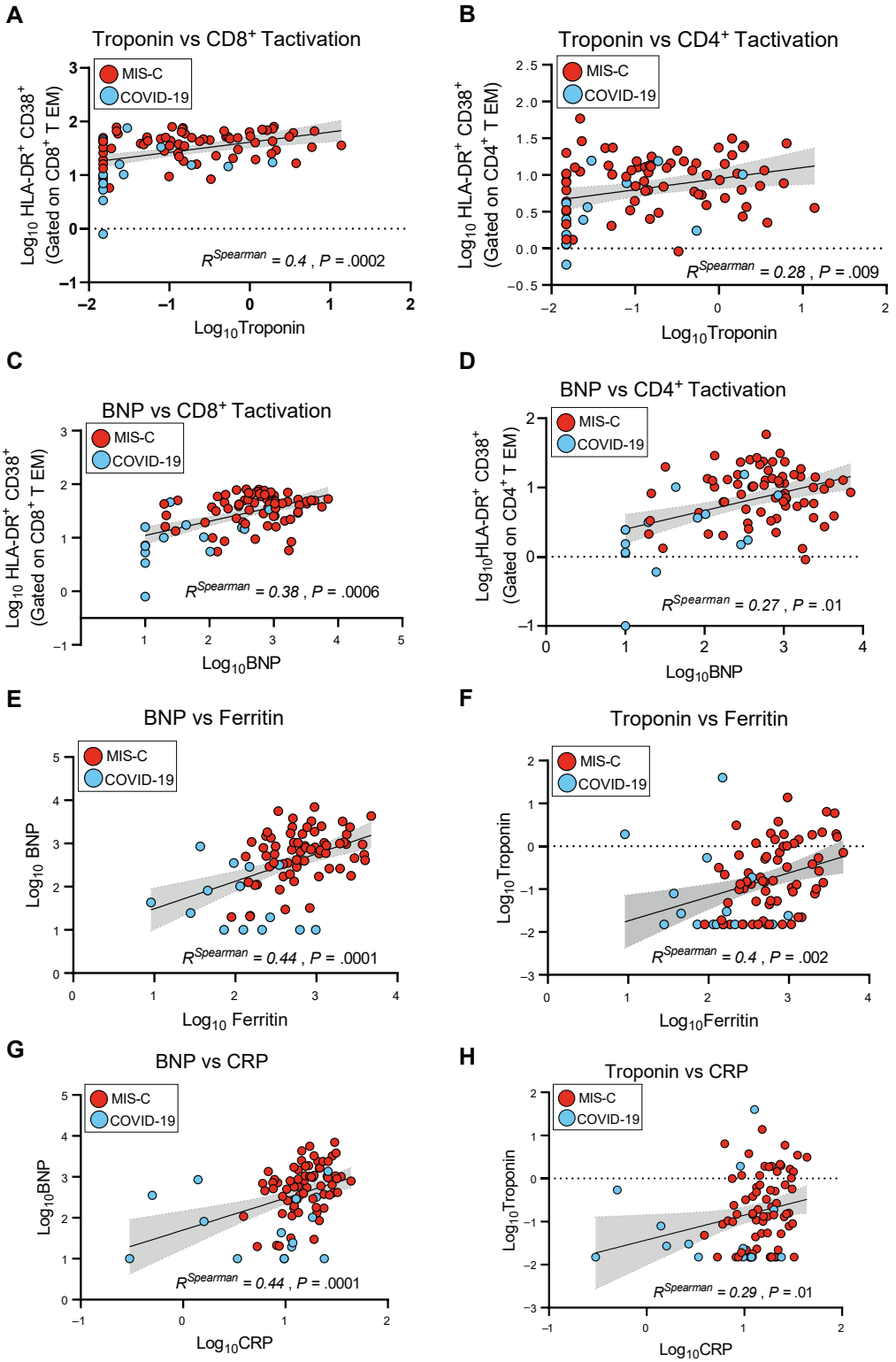

FIG 5. Cardiac dysfunction markers correlate with T-cell activation in patients with MIS-C and COVID-19. **A-D,** Scatter plots showing correlation of serum BNP and troponin levels with $CD8^+$ and $CD4^+$ EM T-cell activation. **E-H,** Scatter plots showing correlation of serum BNP and troponin levels with ferritin and CRP. Spearman correlation coefficient and *P* values are indicated.

(>0.09 ng/mL) levels than the patients who had lower T-cell activation. This suggests that T-cell activation might directly or indirectly contribute to cardiac pathology with elevation of BNP and troponin levels in these children with MIS-C.

We also correlated other inflammatory markers with cardiac dysfunction markers in patients with MIS-C and COVID-19. Ferritin and CRP levels correlated with both BNP and troponin levels (Fig 5, *E-H*). Ferritin and CRP levels also correlated with $CD8^+$ EM T-cell activation (Fig 6, *C*). Thrombocytopenia was frequent in MIS-C. We observed in patients with MIS-C and COVID-19 platelet counts were inversely correlated with $CD4^+$ and $CD8^+$ EM T-cell activation (Fig 6, *A* and *B*). In addition to T-cell activation, other inflammatory markers such as ferritin levels correlated with elevation of liver enzyme alanine transaminase and creatinine, but inversely correlated with platelet count in these patients (Fig 6, *C*). We also compared these parameters separately in patients with MIS-C and patients with COVID-19. Because steroid treatment might affect some of activation readout and laboratory features over time, we evaluated patients with MIS-C in whom sampling was done either presteroids or within the first 48 hours of steroid initiation. We found similar correlations in patients with MIS-C as observed in patients with MIS-C and COVID-19. However, because of the limited number of patients with COVID-19, we observed much lesser correlations between these variables (Fig E10).

DISCUSSION

MIS-C is an immune dysregulation state characterized by hyperinflammation, with multisystem manifestations including myocarditis, cardiac dysfunction, respiratory failure, acute kidney injury, or gastrointestinal, dermatologic, or neurological involvement.[1,17,26,41] Initially, MIS-C was identified in children, but later a similar presentation was also reported in adults.[42-44] Although several groups have demonstrated an increase in inflammatory markers and T-cell activation in MIS-C,[11,28,31,45,46] the exact nature and amplitude of hyperinflammation is still poorly defined. Hence, a comparison with an established hyperinflammatory state such as HLH offers additional insight into the immunopathogenesis of MIS-C. A number of similarities exist, but there are also qualitative and quantitative differences in clinical presentation and management of patients with MIS-C and patients with HLH. For example, hyperinflammation in MIS-C has been treated with steroids, and anakinra.[16,47] Similar cytokine blockade and steroids are used for the management of patients with secondary forms of HLH.[48] Although there are similarities between MIS-C and HLH, they differ in some clinical manifestations such as presence of myocarditis leading to cardiac dysfunction, and gastrointestinal manifestation such as acute abdomen or inflammatory bowel disease–like presentations, which are common in MIS-C but usually not a part of the disease process in HLH.[14,48] In addition, pancytopenia and liver function test abnormities are more commonly seen in HLH but are infrequent in MIS-C. We hypothesized that despite certain clinical similarities, the amplitude and nature of hyperinflammation might be different in MIS-C when compared with HLH.

We found several similarities as well as striking differences between MIS-C and HLH. High T-cell activation was found in both MIS-C and HLH; however, the degree of T-cell activation was lower in MIS-C when compared with HLH. Despite the higher T-cell activation in HLH, we found some patients with MIS-C having $CD8^+$ EM T-cell activation comparable to that seen in patients with HLH. Although CD4 versus CD8 ratio was similar in MIS-C and HLH, high $CD8^+$ EM/naive ratio was observed in HLH, but not in MIS-C, suggesting more dramatic EM T-cell expansion in HLH. Children with COVID-19 had a modest increase in T-cell activation, this finding was not universal in all hospitalized children with COVID-19. In fact, most of these children had only modest T-cell activation when compared with controls, suggesting that unlike in MIS-C, T-cell activation may not be an important driver of disease morbidity in COVID-19 in children. Though we have shown upregulation of surface markers of exhaustion and senescence in T cells, the fact that they resolve during follow-up could suggest that a post-activation state induced transient upregulation of exhaustion markers rather than true exhaustion of T cells.[49] Similarly, transient proliferative stress in the EM compartment of T cells could be the cause of upregulation of senescence marker.

Despite increased T-cell activation in MIS-C, the qualitative nature of T-cell activation is still poorly understood. Hence, we performed additional evaluation of plasma cytokines and chemokines in all patient cohorts. We found elevated plasma IFN-γ and associated chemokines (ie, CXCL9, CXCL10) in both MIS-C and HLH. Interestingly, differences in the degree of T-cell activation were also seen at the cytokine levels where median values for IFN-γ, CXCL9, and CXCL10 were high in HLH when compared with MIS-C. In addition to these cytokines, elevated IL-6 and TNF might be responsible for amplifying the cytokine storm in patients with MIS-C. Innate inflammation can also be a driver of T-cell activation.[50,51] Elevated innate inflammatory cytokines such as IL-18, IL-15, IL-1α, and IL-1RA in MIS-C suggest that innate inflammatory pathways upregulation could play a role in modulating the T-cell activation noted in MIS-C.

Steroids and intravenous immunoglobulin remain the mainstay of therapy for MIS-C.[15,16,52] However, additional biologics were needed for a subset of severely ill patients. Anakinra, tocilizumab, and infliximab are among the common biologics used in the steroid-refractory settings.[27,53-55] Increase in plasma IL-1RA[56] and IL-18[57,58] in patients with MIS-C suggest the significant autoinflammatory component of this disease and reinforces the use of IL-1–blockade therapies such as anakinra in MIS-C.[59] Increase in innate inflammatory signature and elevation of IL-6 and TNF in children with MIS-C noted in our study and previous reports could support the use of IL-6 and TNF blockade.[28,45,46,55,60] Because these biologics are broadly used even in adults with severe COVID-19,[61-63] medication shortages have become a concern. In this context, expanding our armamentarium of drugs available to manage MIS-C hyperinflammation would be advantageous. Agents such as Janus kinase and signal transducer and activator of transcription inhibitors have been used in both HLH and severe COVID-19.[64-68] Given the overlapping hyperinflammation with HLH, similar strategies might be beneficial in patients with MIS-C and further studies are warranted. Similarly, IFN-γ–neutralizing antibody emapalumab has demonstrated efficacy in the management of HLH,[69] and it is currently being evaluated for the management of severe COVID-19 (NCT04324021). Based on our data and previous findings of elevated INF-γ and its chemokines,[28,55] emapalumab might also be another potential agent of interest to evaluate in the management of severe or refractory MIS-C.

We found some unique disease-defining markers in both MIS-C and HLH. For example, cytokines responsible for elevated T_H2

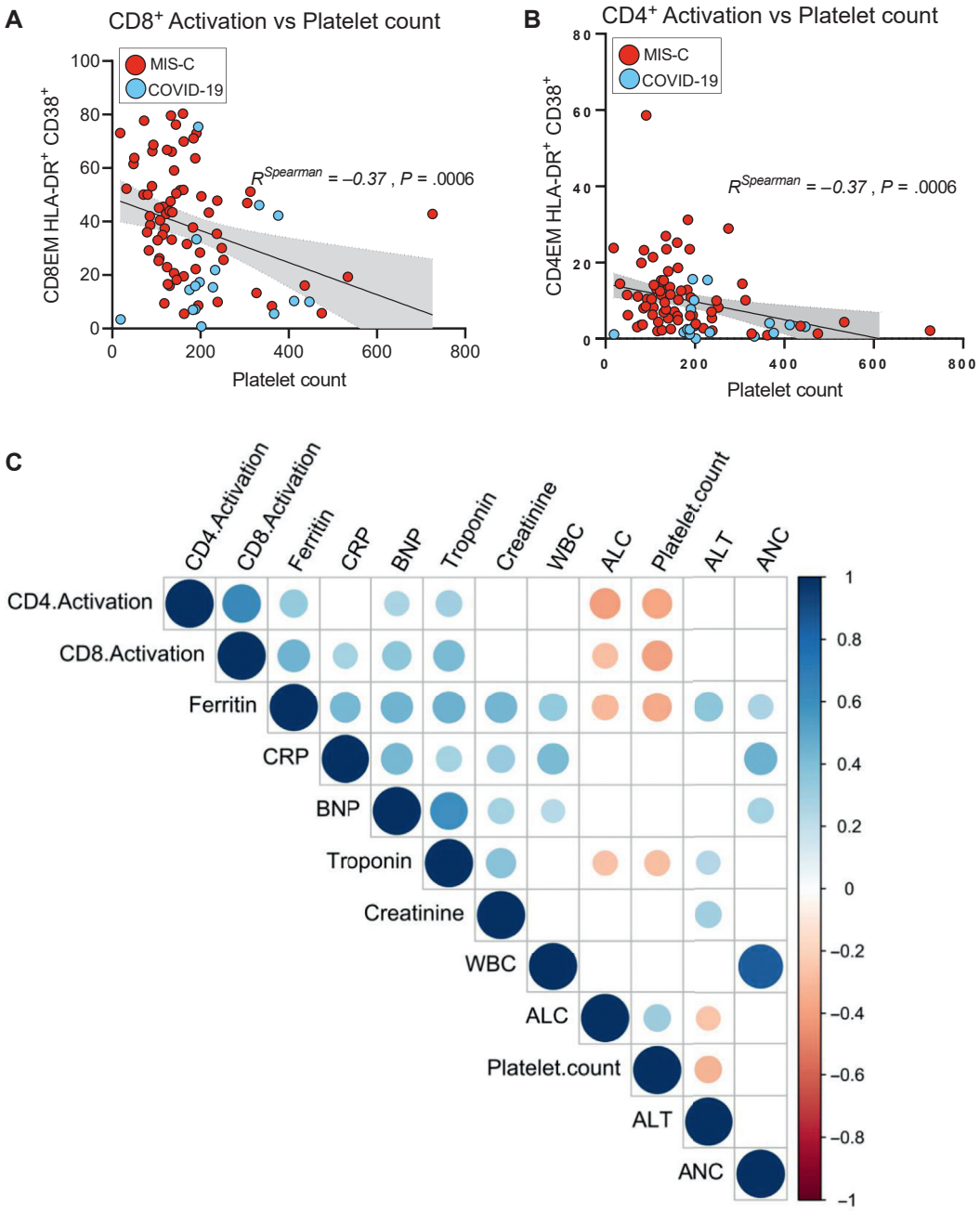

FIG 6. Correlation of laboratory features and immune activation markers in MIS-C and COVID-19. **A** and **B,** Plots showing inverse correlation between platelets and T-cell activation. Spearman's correlation coefficient and *P* values are shown. **C,** Correlation matrix showing positive and inverse correlations between different clinical parameters in patients with COVID-19 and patients with MIS-C. *ALC,* Absolute lymphocyte count; *ALT,* alanine transaminase; *ANC,* absolute neutrophil count; *WBC,* white blood cell. Positive correlation is shown as blue-colored circles, whereas inverse correlation is shown as red-colored circles. Size and intensity of colored circles show the strength of correlation. Only significant correlations with *P* less than .05 are shown as colored circles.

inflammation, IL-4 and IL-13, were uniquely elevated in the MIS-C cohort but not in patients with HLH. Similarly, VEGF-A, PDGF-AA, PDGF-AA/AB, and FGF-2, which mainly contribute to angiogenesis, vascular injury, tissue repair, and healing, were found elevated in MIS-C and not in HLH. Elevated VEGF-A levels and angiogenesis have been shown to be involved in cardiovascular diseases.[70,71] Thrombotic microangiopathy (TMA) has been reported as an important part of pathophysiology in patients with COVID-19 and MIS-C,[72-76] and its etiology is likely multifactorial. Complement dysregulation characterized by IFN-γ signature, elevated soluble C5b9, and TMA is noted in both HLH and MIS-C.[75-77] In addition to complement

dysregulation, elevated VEGF levels might contribute to TMA-like phenotype in MIS-C. Previous literature from other systemic inflammatory diseases showed that increase in VEGF might contribute to TMA.[78,79] Elevated VEGF might be related to high angiotensin II (AngII) from dysregulation of physiological balance of angiotensin-converting enzyme 2-angiotensin II pathway caused by SARS-COV-2 infection. Increased AngII is known to increase VEGF expression and levels[80,81]; together, they could contribute to endothelial activation and dysfunction. It is possible that angiotensin-converting enzyme 2-angiotensin II dysregulation persists in MIS-C after initial infection of SARS-COV-2, hence contributing to microangiopathy and organ injury. In addition to complement dysregulation and VEGF contributing to TMA, platelet activation as evident by increase in plasma PDGF levels[82] may lead to platelet aggregation and consumption and contribute to thrombocytopenia and microangiopathy.[83]

Despite higher T-cell activation in HLH, significant cardiac dysfunction is uncommon. Elevation of troponin as well as VEGF-A in MIS-C but not in HLH suggests increased angiogenetic inflammation. Also, cardiac dysfunction along with T_H2 phenotype might drive an antibody-driven vasculitis-like process in patients with MIS-C. The observation of concomitant T_H2 activation and increase in angiogenic inflammatory markers might explain why most patients with HLH do not develop this degree of myocarditis and gastrointestinal vasculopathy when compared with patients with MIS-C. This suggests that although the nature of T-cell activation in HLH is overwhelmingly T_H1 biased, in MIS-C, it is both T_H1 and T_H2. Moreover, the tropism of activated T cells might be different. In HLH, the tropism might be directed more to the bone marrow, liver, and other lymphoid organs, leading to more pancytopenia, liver dysfunction, and organomegaly, whereas in MIS-C, it might be directed more toward the heart, the gastrointestinal tract, and vascular inflammation.

Our correlation data revealed that global markers of inflammation such as ferritin and CRP are predictive markers of cardiac morbidity. In addition, more specific T-cell activation was shown to significantly correlate with cardiac inflammatory markers, suggesting a role of T-cell activation in cardiac and systemic manifestations in MIS-C. Such global markers of inflammation can also be used to track the disease course in these patients. Furthermore, most patients with MIS-C even at 2-month follow-up were found to have T-cell activation and cytokine and chemokine milieu comparable to that in HCs, suggesting that hyperinflammation in MIS-C caused by cytokine storm is transient, amenable to be controlled by therapies, and almost universally resolves with time.

Our study had a few limitations, and future studies are needed to further strengthen these observations. Because of its rarity, we could include only a limited number of patients with HLH. In future studies, these observations can be compared with a larger cohort of patients with HLH. Many patients with MIS-C had received some immunosuppressive intervention such as steroids before study enrollment. However, the high acuity of clinical presentation of patients with MIS-C and need to start immunomodulatory interventions immediately precludes access to biological samples of truly treatment-naive patients. These practical limitations were noted in other MIS-C and HLH studies describing immune activation and dysregulation.[20,31] To minimize the effect of these interventions, most patients in our study were enrolled either pretherapy or within the first couple of days of steroid initiation, thus minimizing the effect of therapy on the research observations. Nonetheless, future studies focused on treatment-naive cohorts with MIS-C would be more desirable.

CONCLUSIONS

In this study, we characterized the similarities and differences in hyperinflammatory states of MIS-C and HLH. We found high T-cell activation and T_H1-type inflammation in both MIS-C and HLH; however, the amplitude of T-cell activation and T_H1 cytokines was higher in HLH versus MIS-C. In addition to T_H1, elevation of T_H2-type and angiogenic cytokines and chemokines was unique to MIS-C. We also found that T-cell activation as well as other clinical parameters such as ferritin and CRP correlated with cardiac dysfunction markers. Importantly, the hyperinflammation in MIS-C was transient and resolved at follow-up. Overall, our data revealed a comprehensive comparison elucidating both shared features and differences in immune signatures that might help guide treatment strategies for these distinct clinical entities.

Emory + Children's (Pediatric) Flow Cytometry Core facility was used for flow cytometry studies.

Clinical implications: Although the hyperinflammatory profiles of MIS-C and HLH overlap, they differ in amplitude and qualitative nature of immune activation. Global markers of inflammation and $CD8^+$ EM T-cell activation markers correlate with cardiac morbidity in MIS-C. The inflammatory milieu in MIS-C resolves during follow-up.

REFERENCES

1. Feldstein LR, Rose EB, Horwitz SM, Collins JP, Newhams MM, Son MBF, et al. Multisystem inflammatory syndrome in U.S. children and adolescents. N Engl J Med 2020;383:334-46.
2. Brodin P. Why is COVID-19 so mild in children? Acta Paediatr 2020;109:1082-3.
3. Payne AB, Gilani Z, Godfred-Cato S, Belay ED, Feldstein LR, Patel MM, et al. Incidence of multisystem inflammatory syndrome in children among US persons infected with SARS-CoV-2. JAMA Netw Open 2021;4:e2116420.
4. Riphagen S, Gomez X, Gonzalez-Martinez C, Wilkinson N, Theocharis P. Hyperinflammatory shock in children during COVID-19 pandemic. Lancet 2020;395:1607-8.
5. Jiang L, Tang K, Levin M, Irfan O, Morris SK, Wilson K, et al. COVID-19 and multisystem inflammatory syndrome in children and adolescents. Lancet Infect Dis 2020;20:e276-88.
6. Dufort EM, Koumans EH, Chow EJ, Rosenthal EM, Muse A, Rowlands J, et al. Multisystem inflammatory syndrome in children in New York State. N Engl J Med 2020;383:347-58.
7. Lee MS, Liu YC, Tsai CC, Hsu JH, Wu JR. Similarities and differences between COVID-19-related multisystem inflammatory syndrome in children and Kawasaki disease. Front Pediatr 2021;9:640118.
8. Sperotto F, Friedman KG, Son MBF, VanderPluym CJ, Newburger JW, Dionne A. Cardiac manifestations in SARS-CoV-2-associated multisystem inflammatory syndrome in children: a comprehensive review and proposed clinical approach. Eur J Pediatr 2021;180:307-22.
9. Tacke CE, Breunis WB, Pereira RR, Breur JM, Kuipers IM, Kuijpers TW. Five years of Kawasaki disease in the Netherlands: a national surveillance study. Pediatr Infect Dis J 2014;33:793-7.
10. Nakra NA, Blumberg DA, Herrera-Guerra A, Lakshminrusimha S. Multi-system inflammatory syndrome in children (MIS-C) following SARS-CoV-2 infection: review of clinical presentation, hypothetical pathogenesis, and proposed management. Children (Basel) 2020;7:69.

11. Consiglio CR, Cotugno N, Sardh F, Pou C, Amodio D, Rodriguez L, et al. The immunology of multisystem inflammatory syndrome in children with COVID-19. Cell 2020;183:968-81.e7.
12. Hennon TR, Yu KOA, Penque MD, Abdul-Aziz R, Chang AC, McGreevy MB, et al. COVID-19 associated multisystem inflammatory syndrome in children (MIS-C) guidelines; a Western New York approach as the pandemic evolves. Prog Pediatr Cardiol 2021;62:101407.
13. Henter JI, Horne A, Aricó M, Egeler RM, Filipovich AH, Imashuku S, et al. HLH-2004: diagnostic and therapeutic guidelines for hemophagocytic lymphohistiocytosis. Pediatr Blood Cancer 2007;48:124-31.
14. Chandrakasan S, Filipovich AH. Hemophagocytic lymphohistiocytosis: advances in pathophysiology, diagnosis, and treatment. J Pediatr 2013;163:1253-9.
15. Son MBF, Murray N, Friedman K, Young CC, Newhams MM, Feldstein LR, et al. Multisystem inflammatory syndrome in children—initial therapy and outcomes. N Engl J Med 2021;385:23-34.
16. Ouldali N, Toubiana J, Antona D, Javouhey E, Madhi F, Lorrot M, et al. Association of intravenous immunoglobulins plus methylprednisolone vs immunoglobulins alone with course of fever in multisystem inflammatory syndrome in children. JAMA 2021;325:855-64.
17. Centers for Disease Control and Prevention 2020. Multisystem inflammatory syndrome in children (MIS-C) associated with coronavirus disease 2019 (COVID-19). Available at: https://emergency.cdc.gov/han/2020/han00432.asp. Accessed May 14, 2020.
18. Khandelwal P, Chaturvedi V, Owsley E, Lane A, Heyenbruch D, Lutzko CM, et al. CD38(bright)CD8(+) T cells associated with the development of acute GVHD are activated, proliferating, and cytotoxic trafficking cells. Biol Blood Marrow Transplant 2020;26:1-6.
19. Khandelwal P, Lane A, Chaturvedi V, Owsley E, Davies SM, Marmer D, et al. Peripheral blood CD38 bright CD8+ effector memory T cells predict acute graft-versus-host disease. Biol Blood Marrow Transplant 2015;21:1215-22.
20. Chaturvedi V, Marsh RA, Lorenz AZ, Owsley E, Chaturvedi V, Nguyen T, et al. T cell activation profiles distinguish hemophagocytic lymphohistiocytosis and early sepsis. Blood 2021;137:2337-46.
21. Anderson AC, Joller N, Kuchroo VK. Lag-3, Tim-3, and TIGIT: co-inhibitory receptors with specialized functions in immune regulation. Immunity 2016;44:989-1004.
22. Cura Daball P, Ventura Ferreira MS, Ammann S, Klemann C, Lorenz MR, Warthorst U, et al. CD57 identifies T cells with functional senescence before terminal differentiation and relative telomere shortening in patients with activated PI3 kinase delta syndrome. Immunol Cell Biol 2018;96:1060-71.
23. Lopez-Vergès S, Milush JM, Pandey S, York VA, Arakawa-Hoyt J, Pircher H, et al. CD57 defines a functionally distinct population of mature NK cells in the human CD56dimCD16+ NK-cell subset. Blood 2010;116:3865-74.
24. Focosi D, Bestagno M, Burrone O, Petrini M. CD57+ T lymphocytes and functional immune deficiency. J Leukoc Biol 2010;87:107-16.
25. Brenchley JM, Karandikar NJ, Betts MR, Ambrozak DR, Hill BJ, Crotty LE, et al. Expression of CD57 defines replicative senescence and antigen-induced apoptotic death of CD8+ T cells. Blood 2003;101:2711-20.
26. Feldstein LR, Tenforde MW, Friedman KG, Newhams M, Rose EB, Dapul H, et al. Characteristics and outcomes of US children and adolescents with multisystem inflammatory syndrome in children (MIS-C) compared with severe acute COVID-19. JAMA 2021;325:1074-87.
27. Whittaker E, Bamford A, Kenny J, Kaforou M, Jones CE, Shah P, et al. Clinical characteristics of 58 children with a pediatric inflammatory multisystem syndrome temporally associated with SARS-CoV-2. JAMA 2020;324:259-69.
28. Diorio C, Henrickson SE, Vella LA, McNerney KO, Chase J, Burudpakdee C, et al. Multisystem inflammatory syndrome in children and COVID-19 are distinct presentations of SARS-CoV-2. J Clin Invest 2020;130:5967-75.
29. Kuri-Cervantes L, Pampena MB, Meng W, Rosenfeld AM, Ittner CAG, Weisman AR, et al. Comprehensive mapping of immune perturbations associated with severe COVID-19. Sci Immunol 2020;5:eabd7114.
30. Mathew D, Giles JR, Baxter AE, Oldridge DA, Greenplate AR, Wu JE, et al. Deep immune profiling of COVID-19 patients reveals distinct immunotypes with therapeutic implications. Science 2020;369:eabc8511.
31. Vella LA, Giles JR, Baxter AE, Oldridge DA, Diorio C, Kuri-Cervantes L, et al. Deep immune profiling of MIS-C demonstrates marked but transient immune activation compared to adult and pediatric COVID-19. Sci Immunol 2021;6:eabf7570.
32. Lin H, Scull BP, Goldberg BR, Abhyankar HA, Eckstein OE, Zinn DJ, et al. IFN-γ signature in the plasma proteome distinguishes pediatric hemophagocytic lymphohistiocytosis from sepsis and SIRS. Blood Advances 2021;5:3457-67.
33. Qian L, Yu S, Yin C, Zhu B, Chen Z, Meng Z, et al. Plasma IFN-γ-inducible chemokines CXCL9 and CXCL10 correlate with survival and chemotherapeutic efficacy in advanced pancreatic ductal adenocarcinoma. Pancreatology 2019;19:340-5.
34. Han JH, Suh C-H, Jung J-Y, Ahn M-H, Han MH, Kwon JE, et al. Elevated circulating levels of the interferon-γ–induced chemokines are associated with disease activity and cutaneous manifestations in adult-onset Still's disease. Sci Rep 2017;7:46652.
35. Yonker LM, Gilboa T, Ogata AF, Senussi Y, Lazarovits R, Boribong BP, et al. Multisystem inflammatory syndrome in children is driven by zonulin-dependent loss of gut mucosal barrier. J Clin Invest 2021;131:e149633.
36. Reiff DD, Cron RQ. Performance of cytokine storm syndrome scoring systems in pediatric COVID-19 and multisystem inflammatory syndrome in children. ACR Open Rheumatol 2021;3:820-6.
37. Song CY, Xu J, He JQ, Lu YQ. Immune dysfunction following COVID-19, especially in severe patients. Sci Rep 2020;10:15838.
38. Godfred-Cato S, Bryant B, Leung J, Oster ME, Conklin L, Abrams J, et al. COVID-19-associated multisystem inflammatory syndrome in children—United States, March-July 2020. MMWR Morb Mortal Wkly Rep 2020;69:1074-80.
39. Valverde I, Singh Y, Sanchez-de-Toledo J, Theocharis P, Chikermane A, Di Filippo S, et al. Acute cardiovascular manifestations in 286 children with multisystem inflammatory syndrome associated with COVID-19 infection in Europe. Circulation 2021;143:21-32.
40. Zhao Y, Patel J, Huang Y, Yin L, Tang L. Cardiac markers of multisystem inflammatory syndrome in children (MIS-C) in COVID-19 patients: a meta-analysis. Am J Emerg Med 2021;49:62-70.
41. Miller J, Cantor A, Zachariah P, Ahn D, Martinez M, Margolis KG. Gastrointestinal symptoms as a major presentation component of a novel multisystem inflammatory syndrome in children that is related to coronavirus disease 2019: a single center experience of 44 Cases. Gastroenterology 2020;159:1571-4.e2.
42. Morris SB, Schwartz NG, Patel P, Abbo L, Beauchamps L, Balan S, et al. Case series of multisystem inflammatory syndrome in adults associated with SARS-CoV-2 infection—United Kingdom and United States, March-August 2020. MMWR Morb Mortal Wkly Rep 2020;69:1450-6.
43. Weatherhead JE, Clark E, Vogel TP, Atmar RL, Kulkarni PA. Inflammatory syndromes associated with SARS-CoV-2 infection: dysregulation of the immune response across the age spectrum. J Clin Invest 2020;130:6194-7.
44. Shaigany S, Gnirke M, Guttmann A, Chong H, Meehan S, Raabe V, et al. An adult with Kawasaki-like multisystem inflammatory syndrome associated with COVID-19. Lancet 2020;396:e8-10.
45. Gruber CN, Patel RS, Trachtman R, Lepow L, Amanat F, Krammer F, et al. Mapping systemic inflammation and antibody responses in multisystem inflammatory syndrome in children (MIS-C). Cell 2020;183:982-95.e14.
46. Lee PY, Day-Lewis M, Henderson LA, Friedman KG, Lo J, Roberts JE, et al. Distinct clinical and immunological features of SARS-CoV-2-induced multisystem inflammatory syndrome in children. J Clin Invest 2020;130:5942-50.
47. Dove ML, Jaggi P, Kelleman M, Abuali M, Ang JY, Ballan W, et al. Multisystem inflammatory syndrome in children: survey of protocols for early hospital evaluation and management. J Pediatr 2021;229:33-40.
48. Canna SW, Marsh RA. Pediatric hemophagocytic lymphohistiocytosis. Blood 2020;135:1332-43.
49. Wherry EJ, Kurachi M. Molecular and cellular insights into T cell exhaustion. Nat Rev Immunol 2015;15:486-99.
50. Lee H-G, Cho M-Z, Choi J-M. Bystander CD4+ T cells: crossroads between innate and adaptive immunity. Exp Mol Med 2020;52:1255-63.
51. Kim T-S, Shin E-C. The activation of bystander CD8+ T cells and their roles in viral infection. Exp Mol Med 2019;51:1-9.
52. Kaushik S, Aydin SI, Derespina KR, Bansal PB, Kowalsky S, Trachtman R, et al. Multisystem inflammatory syndrome in children associated with severe acute respiratory syndrome coronavirus 2 infection (MIS-C): a multi-institutional study from New York City. J Pediatr 2020;224:24-9.
53. Abdel-Haq N, Asmar BI, Deza Leon MP, McGrath EJ, Arora HS, Cashen K, et al. SARS-CoV-2-associated multisystem inflammatory syndrome in children: clinical manifestations and the role of infliximab treatment. Eur J Pediatr 2021;180:1581-91.
54. Dolinger MT, Person H, Smith R, Jarchin L, Pittman N, Dubinsky MC, et al. Pediatric Crohn disease and multisystem inflammatory syndrome in children (MIS-C) and COVID-19 treated with infliximab. J Pediatr Gastroenterol Nutr 2020;71:153-5.
55. Carter MJ, Fish M, Jennings A, Doores KJ, Wellman P, Seow J, et al. Peripheral immunophenotypes in children with multisystem inflammatory syndrome associated with SARS-CoV-2 infection. Nat Med 2020;26:1701-7.
56. Dinarello CA. Overview of the IL-1 family in innate inflammation and acquired immunity. Immunol Rev 2018;281:8-27.
57. Weiss ES, Girard-Guyonvarc'h C, Holzinger D, de Jesus AA, Tariq Z, Picarsic J, et al. Interleukin-18 diagnostically distinguishes and pathogenically promotes human and murine macrophage activation syndrome. Blood 2018;131:1442-55.

58. de Jesus AA, Hou Y, Brooks S, Malle L, Biancotto A, Huang Y, et al. Distinct interferon signatures and cytokine patterns define additional systemic autoinflammatory diseases. J Clin Invest 2020;130:1669-82.
59. Della Paolera S, Valencic E, Piscianz E, Moressa V, Tommasini A, Sagredini R, et al. Case report: use of anakinra in multisystem inflammatory syndrome during COVID-19 pandemic. Front Pediatr 2021;8:624248.
60. Esteve-Sole A, Anton J, Pino-Ramirez RM, Sanchez-Manubens J, Fumadó V, Fortuny C, et al. Similarities and differences between the immunopathogenesis of COVID-19-related pediatric multisystem inflammatory syndrome and Kawasaki disease. J Clin Invest 2021;131:e144554.
61. Robinson PC, Richards D, Tanner HL, Feldmann M. Accumulating evidence suggests anti-TNF therapy needs to be given trial priority in COVID-19 treatment. Lancet Rheumatol 2020;2:e653-5.
62. Feldmann M, Maini RN, Woody JN, Holgate ST, Winter G, Rowland M, et al. Trials of anti-tumour necrosis factor therapy for COVID-19 are urgently needed. Lancet 2020;395:1407-9.
63. Castelnovo L, Tamburello A, Lurati A, Zaccara E, Marrazza MG, Olivetti M, et al. Anti-IL6 treatment of serious COVID-19 disease: a monocentric retrospective experience. Medicine (Baltimore) 2021;100:e23582.
64. Bronte V, Ugel S, Tinazzi E, Vella A, De Sanctis F, Canè S, et al. Baricitinib restrains the immune dysregulation in patients with severe COVID-19. J Clin Invest 2020;130:6409-16.
65. Kalil AC, Patterson TF, Mehta AK, Tomashek KM, Wolfe CR, Ghazaryan V, et al. Baricitinib plus remdesivir for hospitalized adults with Covid-19. N Engl J Med 2021;384:795-807.
66. Patoulias D, Doumas M, Papadopoulos C, Karagiannis A. Janus kinase inhibitors and major COVID-19 outcomes: time to forget the two faces of Janus! A meta-analysis of randomized controlled trials. Clin Rheumatol 2021;40:4671-4.
67. Vannucchi AM, Sordi B, Morettini A, Nozzoli C, Poggesi L, Pieralli F, et al. Compassionate use of JAK1/2 inhibitor ruxolitinib for severe COVID-19: a prospective observational study. Leukemia 2021;35:1121-33.
68. Ahmed A, Merrill SA, Alsawah F, Bockenstedt P, Campagnaro E, Devata S, et al. Ruxolitinib in adult patients with secondary haemophagocytic lymphohistiocytosis: an open-label, single-centre, pilot trial. Lancet Haematol 2019;6:e630-7.
69. Locatelli F, Jordan MB, Allen C, Cesaro S, Rizzari C, Rao A, et al. Emapalumab in children with primary hemophagocytic lymphohistiocytosis. N Engl J Med 2020; 382:1811-22.
70. Cho ML, Jung YO, Moon YM, Min SY, Yoon CH, Lee SH, et al. Interleukin-18 induces the production of vascular endothelial growth factor (VEGF) in rheumatoid arthritis synovial fibroblasts via AP-1-dependent pathways. Immunol Lett 2006; 103:159-66.
71. Kucukardali Y, Aydogdu S, Ozmen N, Yonem A, Solmazgul E, Ozyurt M, et al. The relationship between severity of coronary artery disease and plasma level of vascular endothelial growth factor. Cardiovasc Revasc Med 2008;9: 66-70.
72. Ma L, Sahu SK, Cano M, Kuppuswamy V, Bajwa J, McPhatter J, et al. Increased complement activation is a distinctive feature of severe SARS-CoV-2 infection. bioRxiv 20212021.02.22.432177.
73. Magro C, Mulvey JJ, Berlin D, Nuovo G, Salvatore S, Harp J, et al. Complement associated microvascular injury and thrombosis in the pathogenesis of severe COVID-19 infection: a report of five cases. Transl Res 2020;220:1-13.
74. Ackermann M, Verleden SE, Kuehnel M, Haverich A, Welte T, Laenger F, et al. Pulmonary vascular endothelialitis, thrombosis, and angiogenesis in Covid-19. N Engl J Med 2020;383:120-8.
75. Diorio C, McNerney KO, Lambert M, Paessler M, Anderson EM, Henrickson SE, et al. Evidence of thrombotic microangiopathy in children with SARS-CoV-2 across the spectrum of clinical presentations. Blood Adv 2020;4:6051-63.
76. Diorio C, Shraim R, Vella LA, Giles JR, Baxter AE, Oldridge DA, et al. Proteomic profiling of MIS-C patients indicates heterogeneity relating to interferon gamma dysregulation and vascular endothelial dysfunction. Nat Commun 2021;12:7222.
77. Gloude NJ, Dandoy CE, Davies SM, Myers KC, Jordan MB, Marsh RA, et al. Thinking beyond HLH: clinical features of patients with concurrent presentation of hemophagocytic lymphohistiocytosis and thrombotic microangiopathy. J Clin Immunol 2020;40:699-707.
78. Lee H, Lee Y, Lo A, Powell L, Shah B. Primarily VEGF-driven etiopathogenesis of Tafro syndrome and fibroblastic reticular cells as a probable Castleman cell—qualitative metasynthesis. Blood 2020;136:27-8.
79. Sun PP, Yu XJ, Wang SX, Zhou XJ, Qu L, Zhang F, et al. Association of vascular endothelial growth factor and renal thrombotic microangiopathy-like lesions in patients with Castleman's disease. Nephrology (Carlton) 2020;25:125-34.
80. Otani A, Takagi H, Oh H, Suzuma K, Matsumura M, Ikeda E, et al. Angiotensin II-stimulated vascular endothelial growth factor expression in bovine retinal pericytes. Invest Ophthalmol Vis Sci 2000;41:1192-9.
81. Funatsu H, Yamashita H, Nakanishi Y, Hori S. Angiotensin II and vascular endothelial growth factor in the vitreous fluid of patients with proliferative diabetic retinopathy. Br J Ophthalmol 2002;86:311-5.
82. Selheim F, Fukami MH, Holmsen H, Vassbotn FS. Platelet-derived-growth-factor-induced signalling in human platelets: phosphoinositide-3-kinase-dependent inhibition of platelet activation. Biochem J 2000;350:469-75.
83. Canzano P, Brambilla M, Porro B, Cosentino N, Tortorici E, Vicini S, et al. Platelet and endothelial activation as potential mechanisms behind the thrombotic complications of COVID-19 patients. JACC Basic Transl Sci 2021;6:202-18.

ANTIBODIES USED IN THIS STUDY

CD3-PerCP/Cy5.5 (Biolegend, Cat. #300430; San Diego, Calif), CD4-PE-Cy7 (BD Biosciences, Cat. #560649; Franklin Lakes, NJ), CD8-BUV395 (BD Biosciences, Cat. #563795), CD45RA-APC (Biolegend, Cat. #304112), CCR7-PE (Biolegend, Cat. #353204), HLA-DR-BV711 (BD Biosciences, Cat. #563696), CD38-BUV496 (BD Biosciences, Cat. #612947), PD-1-BV421 (BD Biosciences, Cat. #562516), CD57-BB515 (BD Biosciences, Cat. #565285), and Tim-3-BV650 (Biolegend, Cat. #345028) antibodies were used for staining cells. Live/dead fixable aqua dead cell stain (Thermofisher, Cat. # L34957; Waltham, Mass) was used to exclude dead cells in the analysis.

REFERENCES

E1. Maecker HT, McCoy JP, Nussenblatt R. Standardizing immunophenotyping for the Human Immunology Project. Nat Rev Immunol 2012;12:191-200.

E2. Khandelwal P, Chaturvedi V, Owsley E, Lane A, Heyenbruch D, Lutzko CM, et al. CD38(bright)CD8(+) T cells associated with the development of acute GVHD are activated, proliferating, and cytotoxic trafficking cells. Biol Blood Marrow Transplant 2020;26:1-6.

E3. Khandelwal P, Lane A, Chaturvedi V, Owsley E, Davies SM, Marmer D, et al. Peripheral blood CD38 bright CD8+ effector memory T cells predict acute graft-versus-host disease. Biol Blood Marrow Transplant 2015;21:1215-22.

E4. Chaturvedi V, Marsh RA, Lorenz AZ, Owsley E, Chaturvedi V, Nguyen T, et al. T cell activation profiles distinguish hemophagocytic lymphohistiocytosis and early sepsis. Blood 2021;137:2337-46.

E5. Focosi D, Bestagno M, Burrone O, Petrini M. CD57+ T lymphocytes and functional immune deficiency. J Leukoc Biol 2010;87:107-16.

E6. Cura Daball P, Ventura Ferreira MS, Ammann S, Klemann C, Lorenz MR, Warthorst U, et al. CD57 identifies T cells with functional senescence before terminal differentiation and relative telomere shortening in patients with activated PI3 kinase delta syndrome. Immunol Cell Biol 2018;96:1060-71.

E7. Lopez-Vergès S, Milush JM, Pandey S, York VA, Arakawa-Hoyt J, Pircher H, et al. CD57 defines a functionally distinct population of mature NK cells in the human CD56dimCD16+ NK-cell subset. Blood 2010;116:3865-74.

E8. Brenchley JM, Karandikar NJ, Betts MR, Ambrozak DR, Hill BJ, Crotty LE, et al. Expression of CD57 defines replicative senescence and antigen-induced apoptotic death of CD8+ T cells. Blood 2003;101:2711-20.

E9. Anderson AC, Joller N, Kuchroo VK. Lag-3, Tim-3, and TIGIT: co-inhibitory receptors with specialized functions in immune regulation. Immunity 2016;44:989-1004.

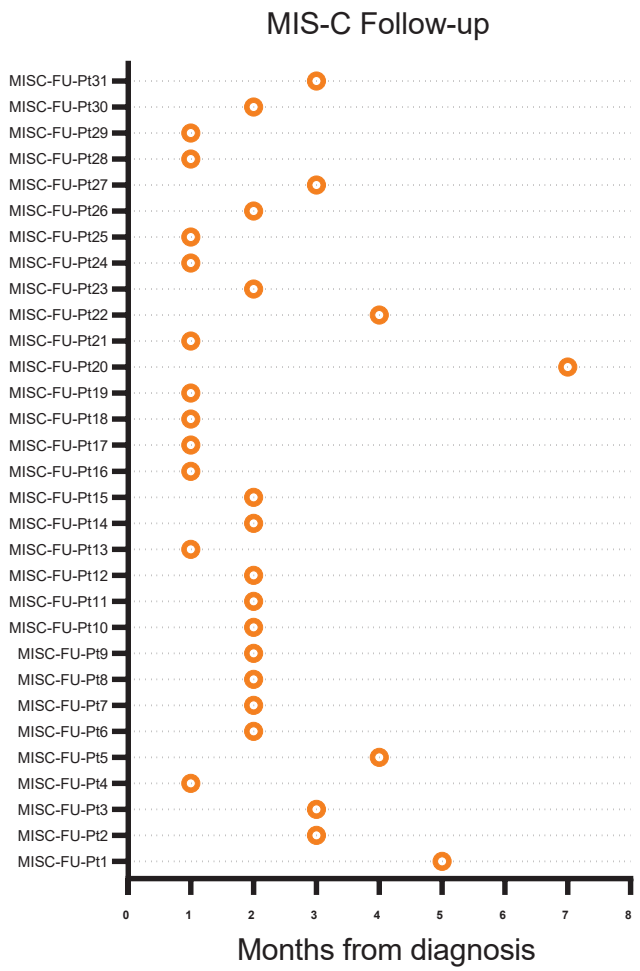

FIG E1. Distribution of follow-up blood sampling of patients with MIS-C. "0" represents the first blood sample drawn, and circles represent when follow-up samples were obtained since initial diagnosis.

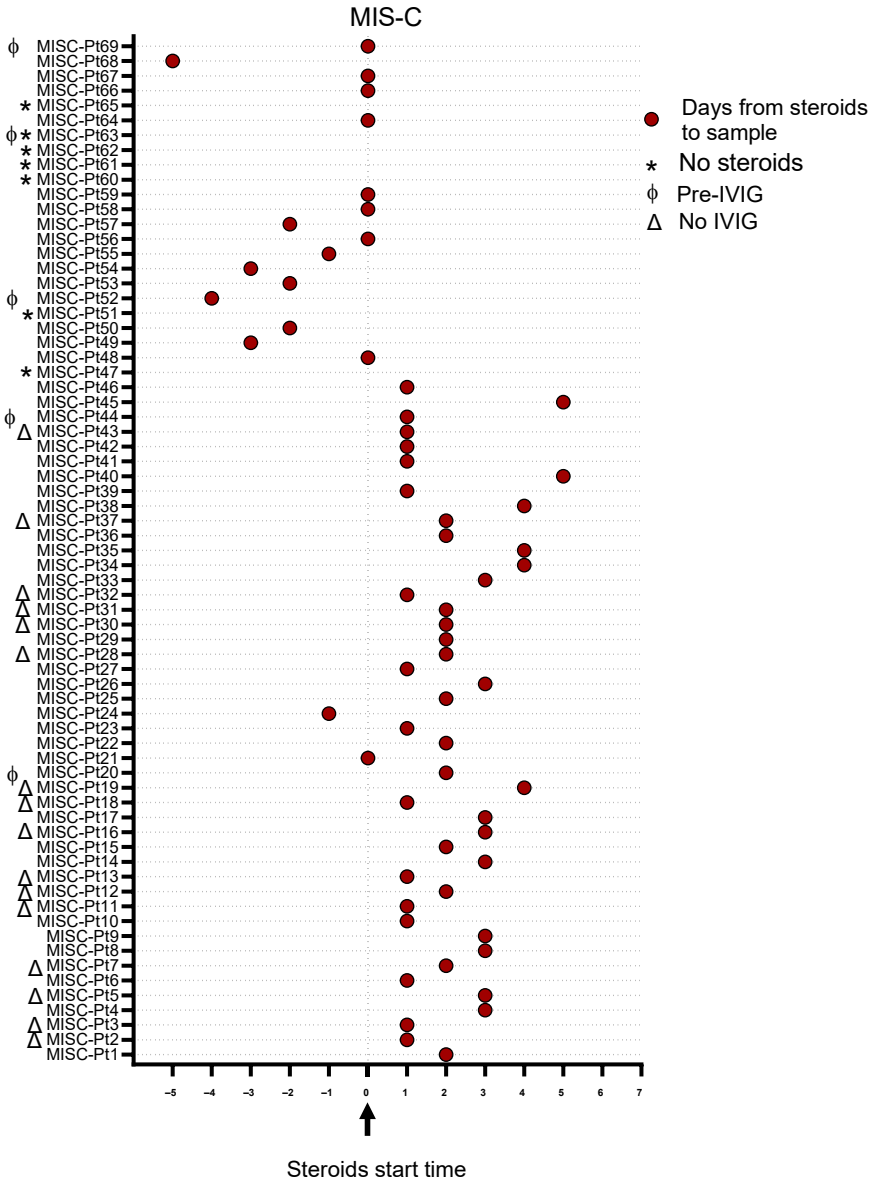

FIG E2. Treatment and blood sampling timeline of patients with MIS-C. Timeline for patients with MIS-C indicating blood sampling with respect to start of steroid treatment (vertical dotted line). *IVIG*, Intravenous immunoglobulin. Each row represents an individual patient with MIS-C. "0" represents blood sampling within first 24 hours of initiation of steroid treatment. "1" represents blood sampling within 24 to 48 hours of steroid initiation and so on. * represents patients with MIS-C who did not receive any steroids during hospital stay. Φ represents patients in whom blood sampling was done before IVIG. Δ represents patients who did not receive IVIG. Rest all patients received IVIG before blood sampling.

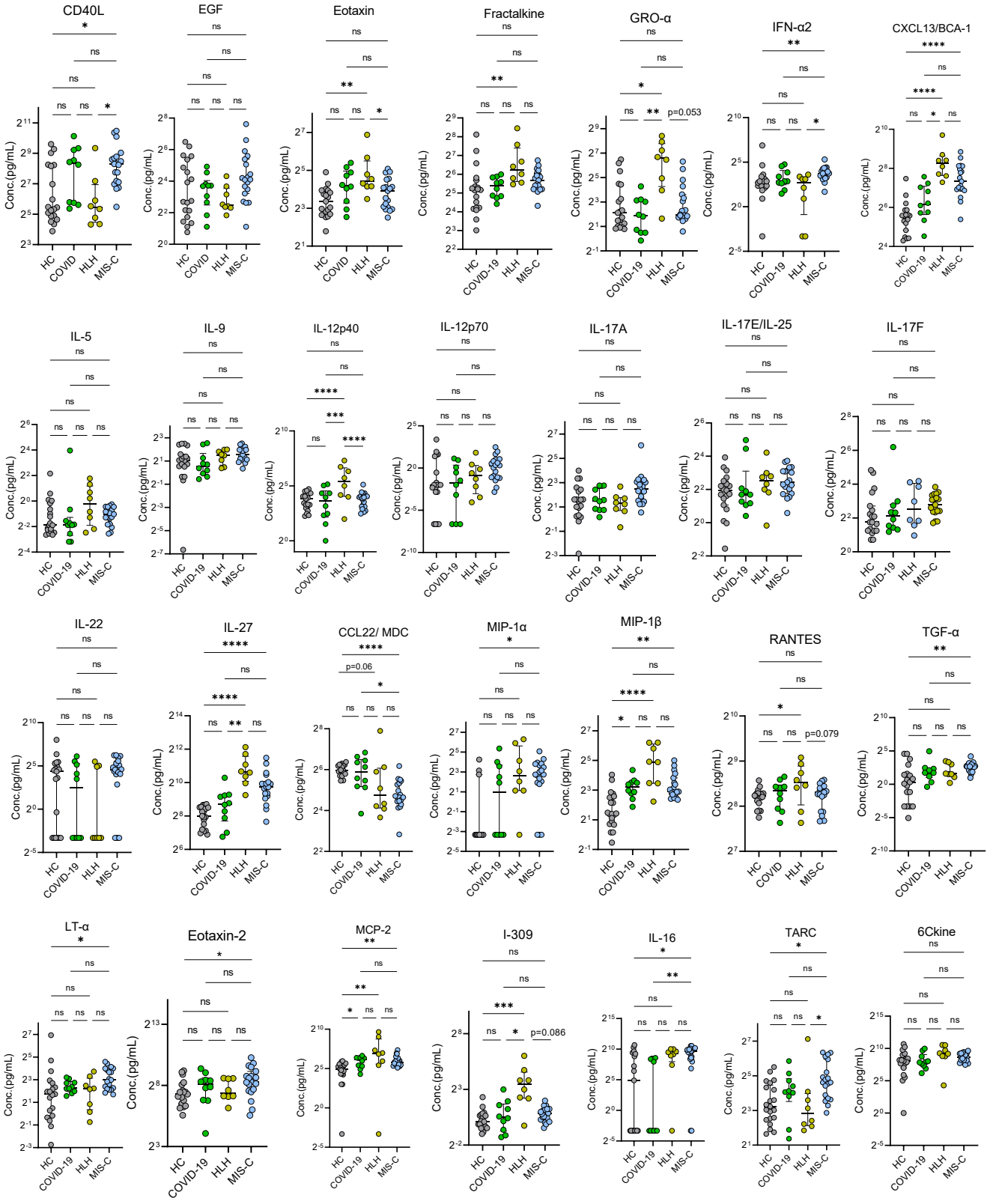

FIG E3. Comparison of serum levels of selected cytokines in different patient groups. Dot plots showing serum concentrations of selected cytokines/chemokines in HCs and patients with COVID-19, patients with HLH, and patients with MIS-C. *Conc.*, Concentration; *ns,* not significant. Kruskal-Wallis 1-way ANOVA followed by Dunn's multiple comparison test for nonnormally distributed samples and ordinary 1-way ANOVA followed by Tukey's multiple comparison test for normally distributed samples were used for statistical comparison. **P* < .05, ***P* < .01, ****P* < .001; *****P* < .0001.

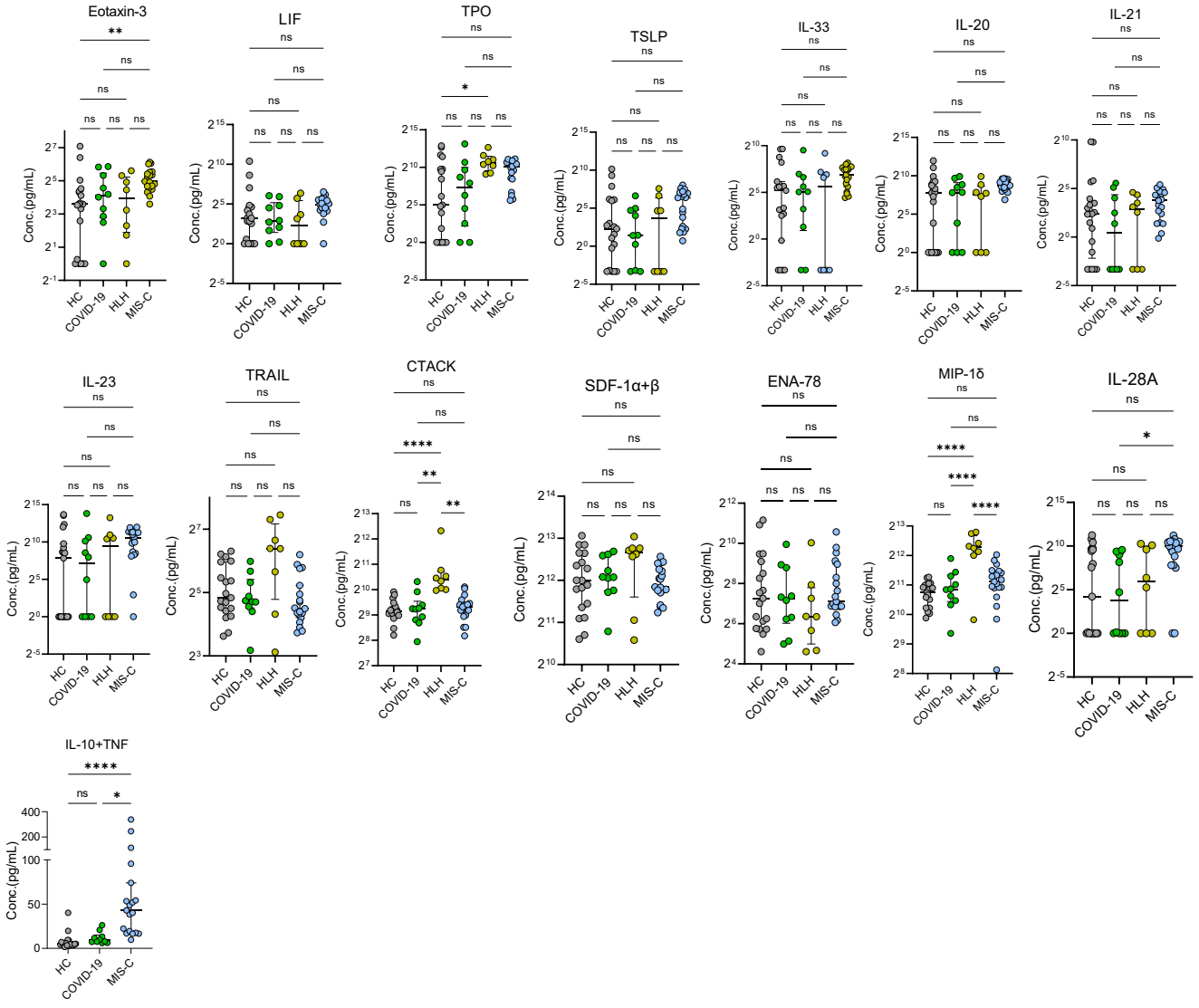

FIG E3. (Continued).

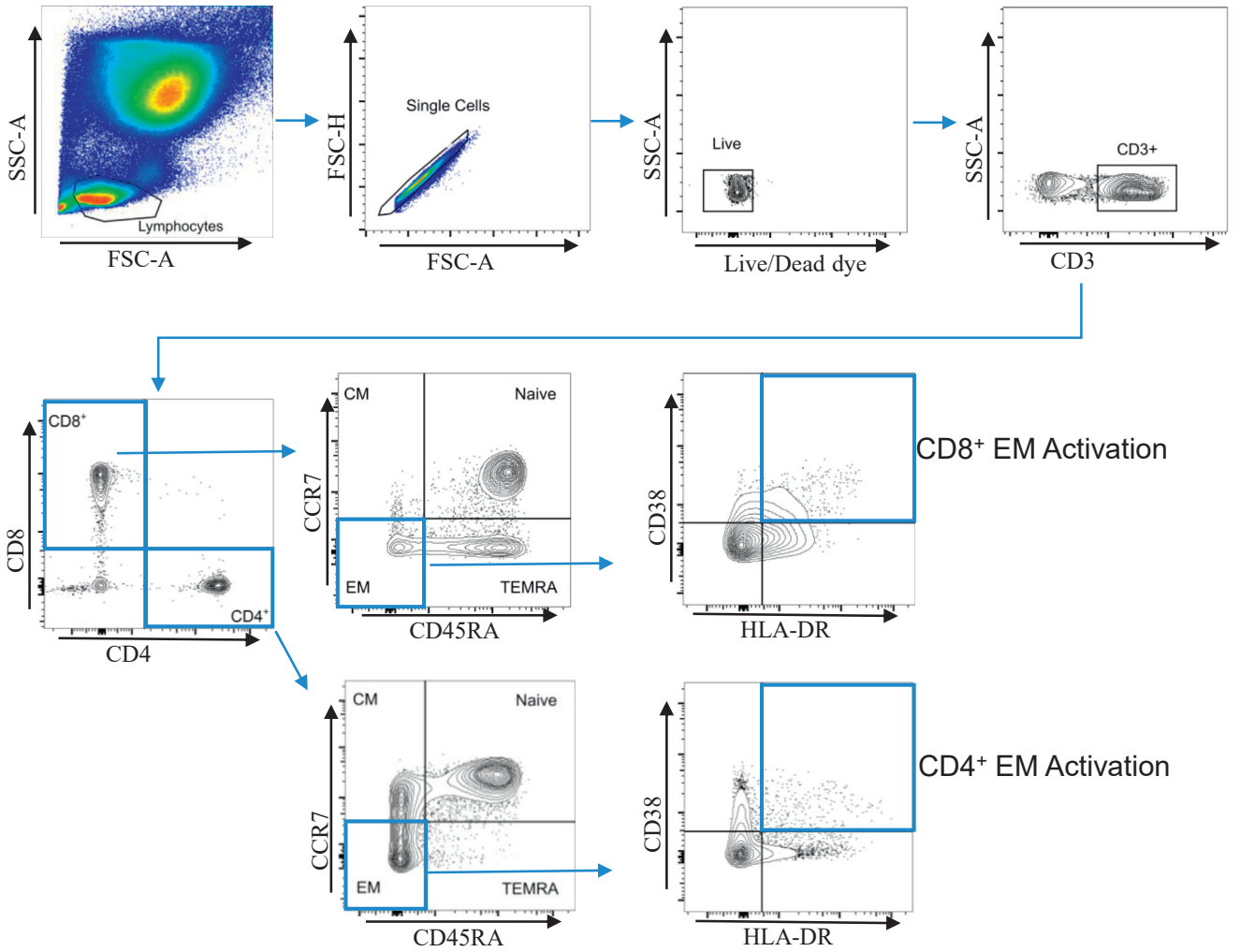

FIG E4. Gating strategy used to define $CD4^+$ and $CD8^+$ T-cell activation in different patient cohorts. *FSC-A*, Forward scatter-area; *FSC-H*, forward scatter-height; *SSC-A*, side scatter-area.

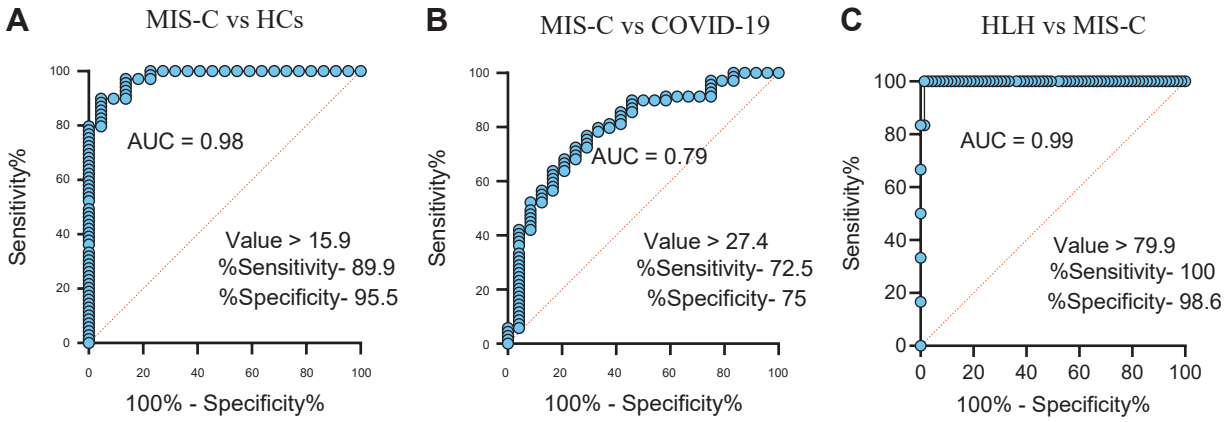

FIG E5. Evaluation of differences in $CD8^+$ EM T-cell activation in patient cohorts. ROC curves showing optimal threshold value with corresponding percentage sensitivity and specificity for frequency of $HLA\text{-}DR^+CD38^+$ on EM $CD8^+$ T cells between HCs vs MIS-C (**A**), MIS-C vs COVID-19 (**B**), and HLH vs MIS-C (**C**). *AUC*, Area under the ROC curve.

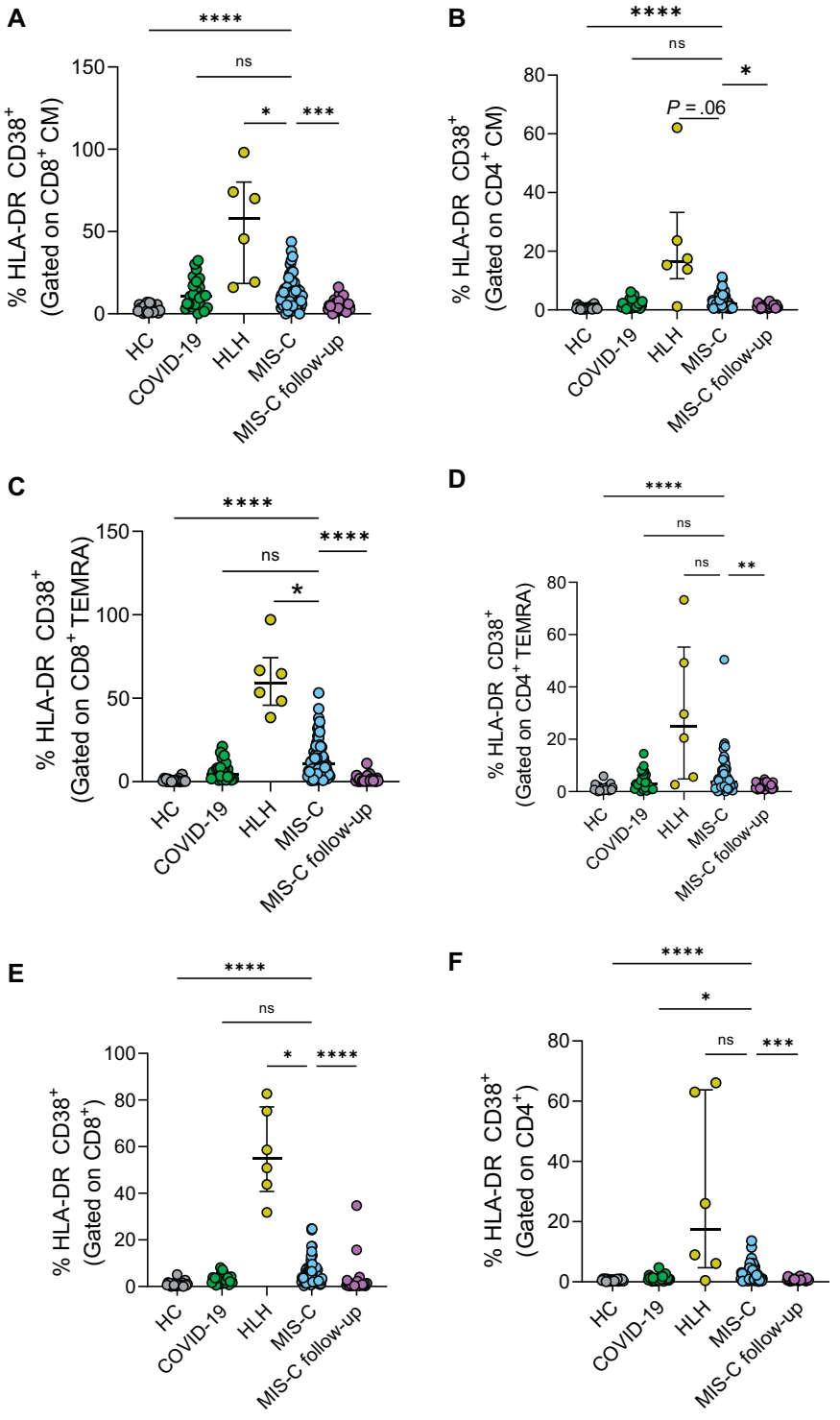

FIG E6. Comparison of T-cell activation in different subsets of $CD8^+$ and $CD4^+$ T-cell populations. Dot plots showing HLA-DR^+ $CD38^+$ coexpression in CM (**A** and **B**) and TEMRA (**C** and **D**) subsets of $CD8^+$ and $CD4^+$ T cells and also on total $CD8^+$ and $CD4^+$ T-cell populations (**E** and **F**). *CM*, Central memory; *ns*, nonsignificant.

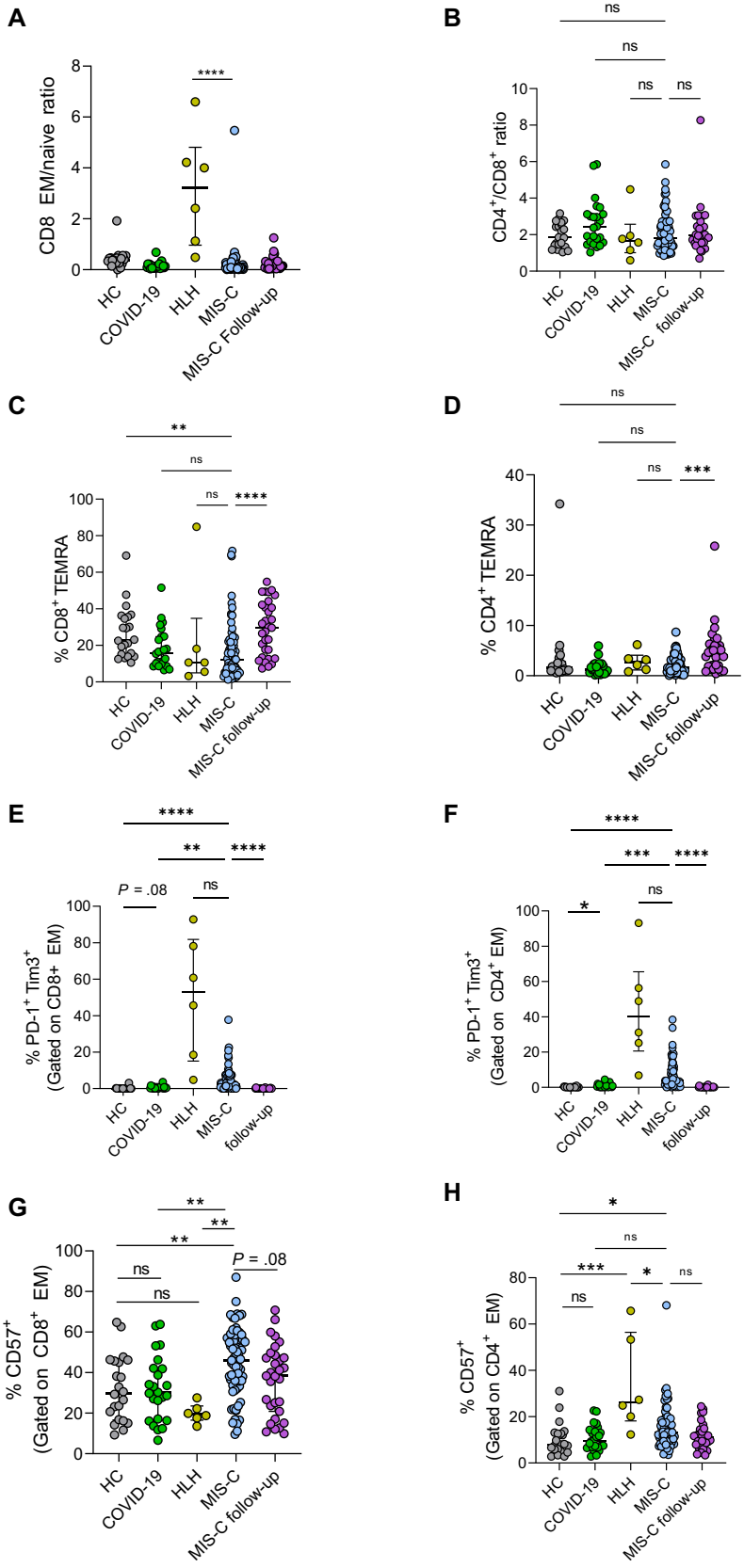

FIG E7. Quantitation of T-cell perturbations among different patient cohorts. (**A**) Plots showing ratio of $CD8^+$ EM vs naive compartment and (**B**) $CD4^+$ vs $CD8^+$ ratio in different patient cohorts. Dot plots showing frequencies of $CD8^+$ and $CD4^+$ TEMRA populations (**C** and **D**). Plots showing percentage coexpression of PD-1^+ and Tim3^+ (**E** and **F**) and expression of $CD57^+$ in the EM compartment of $CD8^+$ and $CD4^+$ T cells (**G** and **H**) in HCs (n = 22) and COVID-19 (n = 24), HLH (n = 6), MIS-C (n = 69), and MIS-C follow-up (n = 31) patients. *ns*, Nonsignificant.

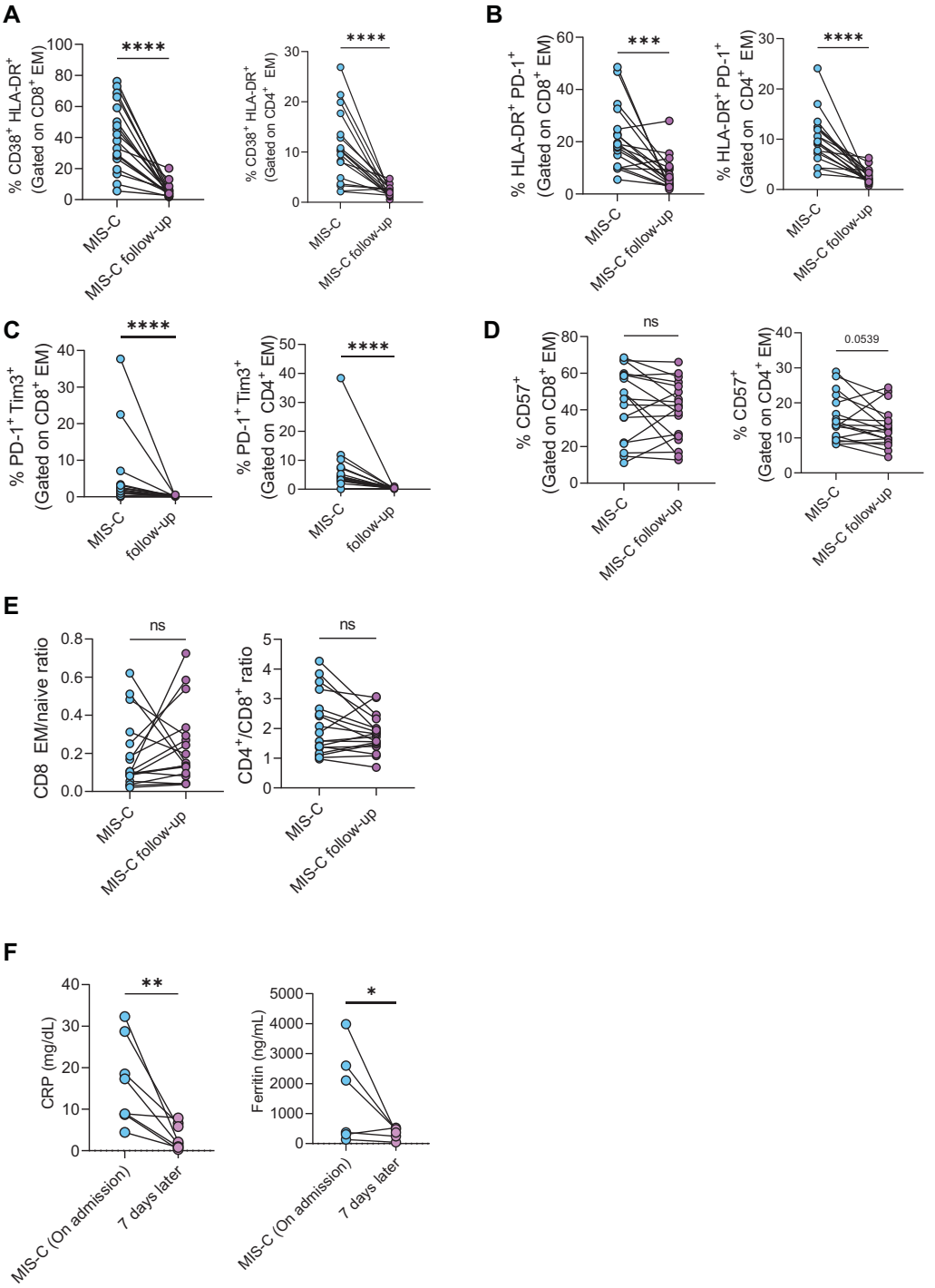

FIG E8. Follow-up analysis of patients with MIS-C displays decrease in activation, exhaustion, and senescence markers on T cells along with improvement in clinical markers of inflammation. **A-E,** Dot plots showing paired analysis of different states of T cells and its subsets in patients with MIS-C at onset and follow-up (n = 18). **F,** Paired analysis of patients with MIS-C showing levels of CRP and ferritin at patient admission and 7 days postadmission. *ns*, Nonsignificant.

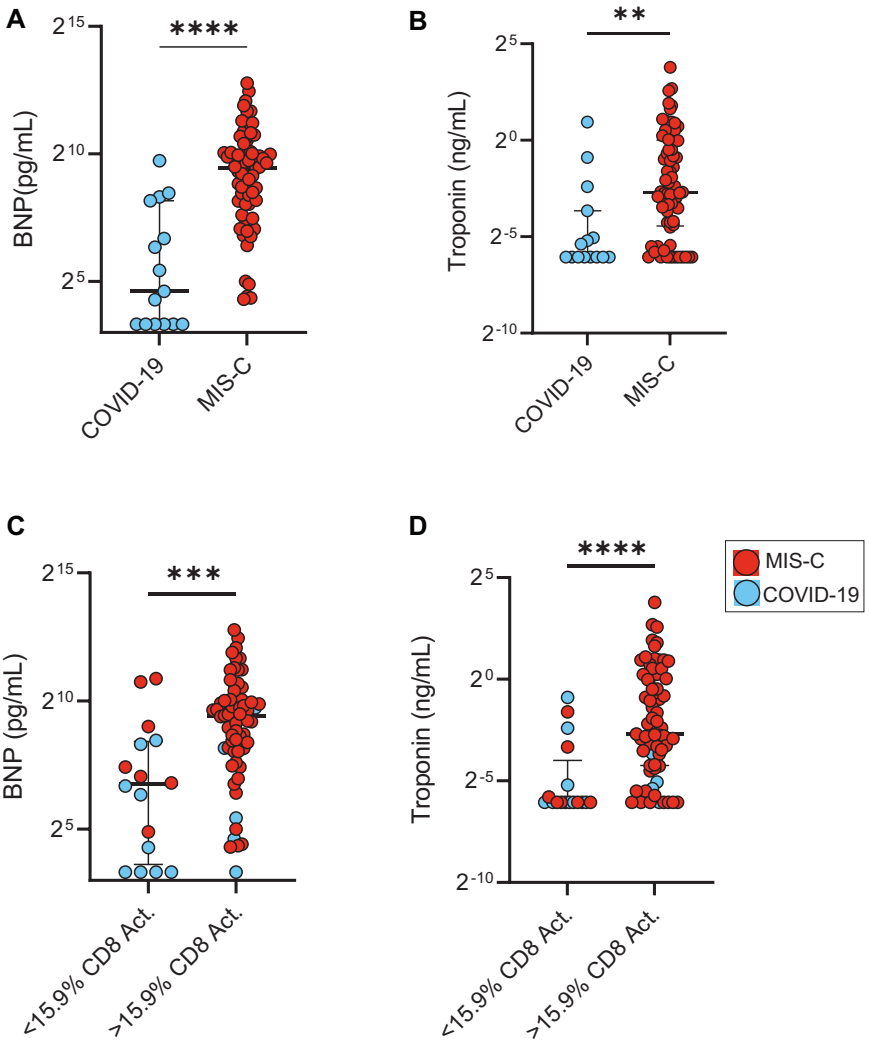

FIG E9. Quantitation of BNP and troponin levels in MIS-C and COVID-19. Plots showing serum levels of BNP (**A**) and troponin (**B**) in patients with COVID-19 (n = 15) and patients with MIS-C (n = 69). Based on % optimal threshold value of $CD8^+$ T activation, patients with MIS-C and patients with COVID-19 were categorized into 2 groups having low (<15.9%) and high $CD8^+$ (>15.9%) EM T-cell activation. Dot plots showing differences between BNP (**C**) and troponin (**D**) levels in groups having low and high $CD8^+$ T-cell activation. *Act.*, Activation.

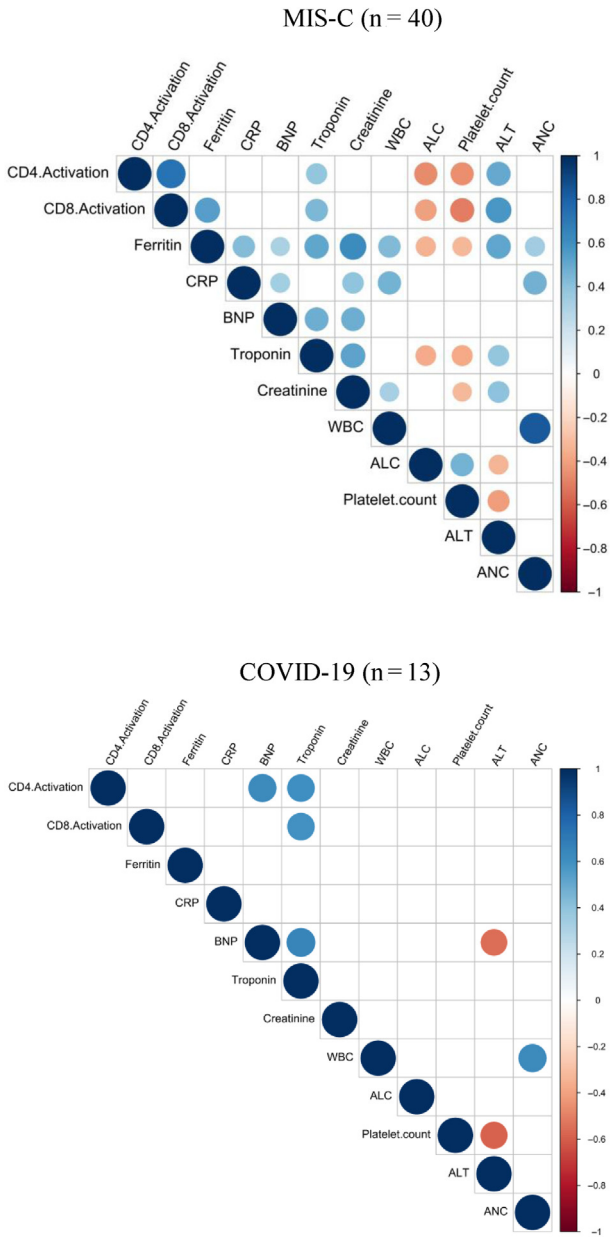

FIG E10. Correlation of laboratory features and immune markers in MIS-C and COVID-19. Correlation matrix showing positive and inverse correlations between different laboratory and immune parameters in patients with COVID-19 (n = 13) and patients with MIS-C (n = 40). Positive correlation is shown as blue-colored circles, whereas inverse correlation is shown in red-colored circles. Size and intensity of colored circles show the strength of correlation. Only significant correlations with *P* less than .05 are shown as colored circles. *ALC*, Absolute lymphocyte count; *ALT*, alanine transaminase; *ANC*, absolute neutrophil count; *WBC*, white blood cell.

TABLE E1. Definitions of different T populations used in this study

Population	Markers	References
CM $CD4^+$ T	$CD4^+$ $CCR7^+$ $CD45RA^-$	E1
CM $CD8^+$ T	$CD8^+$ $CCR7^+$ $CD45RA^-$	E1
EM $CD4^+$ T	$CD4^+$ $CCR7^-$ $CD45RA^-$	E1
EM $CD8^+$ T	$CD8^+$ $CCR7^-$ $CD45RA^-$	E1
TEMRA $CD8^+$T	$CD8^+$ $CCR7^-$ $CD45RA^+$	E1
TEMRA $CD4^+$T	$CD4^+$ $CCR7^-$ $CD45RA^+$	E1
Naive $CD4^+$ T	$CD4^+$ $CCR7^+$ $CD45RA^+$	E1
Naive $CD8^+$ T	$CD8^+$ $CCR7^+$ $CD45RA^+$	E1
Activated $CD4^+$ EM	$CD4^+CD45RA^-CCR7^-$ HLA-DR^+CD38^+	E2-E4
Activated $CD8^+$ EM	$CD8^+CD45RA^-CCR7^-$ HLA-DR^+CD38^+	E2-E4
Senescent $CD4^+$ T	$CD4^+$ $CD45RA^-CCR7^-$ $CD57^+$	E5-E8
Senescent $CD8^+$ T	$CD8^+$ $CD45RA^-CCR7^-$ $CD57^+$	E5-E8
Exhausted $CD4^+$	$CD4^+$ $CD45RA^-CCR7^-$ PD-1^+ $Tim3^+$	E9
Exhausted $CD8^+$	$CD8^+$ $CD45RA^-CCR7^-$ PD-1^+ $Tim3^+$	E9

CM, Central memory.

TABLE E2. List of cytokine and chemokines used for this study

MCP-1	EGF
MCP-3	Eotaxin
M-CSF	FGF-2
CCL22	FLT-3L
MIG/CXCL9	Fractalkine
MIP-1α	G-CSF
MIP-1β	GROα
PDGF-AA	IFN-α2
PDGF-AB/BB	IFN-γ
RANTES	IL-1α
TGF-α	IL-1β
TNF	IL-1RA
LT-α	IL-4
VEGF-A	IL-5
Eotaxin-2	IL-6
MCP-2	IL-8
CXCL13	IL-9
MCP-4	IL-10
I-309	IL-12p40
IL-16	IL-12p70
TARC	IL-13
6CKine	IL-15
Eotaxin-3	IL-17A
LIF	IL-17E/IL-25
TPO	IL-17F
TSLP	IL-18
IL-33	IL-22
IL-20	IL-27
IL-21	IP-10/CXCL10
IL-23	MIP-1δ
TRAIL	IL-28A
CTACK	ENA-78
SDF-1α+β	
sCD40L	

CTACK, Cutaneous T-cell–attracting chemokine; *LT-α*, lymphotoxin-alpha.

TABLE E3. Demographic characteristics and clinical information of patients with HLH

Patient ID	Age	Sex	Causal factor (gene defect)	WBC (cells/μL)	ALC (cells/μL)	ANC (cells/μL)	Hemoglobin (g/L)	Platelets (cells × 10^3/μL)	Ferritin maximum (ng/mL)	sIL-2R (U/ mL)
1	5 mo	M	p-HLH (*STXBP2*)	4,140	2,649	890	79	81	40,000	37,874
2	3 mo	M	p-HLH (*UNC13D*)	6,370	4,650	1,210	82	40	13,672	47,474
3	1 d	F	p-HLH (*STXBP2*)	10,370	6,222	2,177	117	63	12,488	11,165
4	3 mo	M	p-HLH (*RAB27a*)	3,520	2,675	180	72	<10	14,855	44,256
5	2 mo	M	p-HLH (*RAB27a*)	2,600	1,508	390	72	23	5,473	22,268
6	2 y 8 mo	M	Suspected p-HLH*	4,130	950	2,740	81	70	5,753	7,125
7	1 y 4 mo	M	Suspected p-HLH*	890	480	400	112	80	5,067	13,625
8	1 y	M	EBV-HLH	200	160	10	47	<10	150,000	46,723
9	1 y	M	EBV-HLH	1,930	1,022	870	85	82	170,000	10,426
10	19 y 4 mo	F	EBV-HLH	2,390	1,888	300	84	47	29,094	11,849
11	7 y 4 mo	F	EBV-HLH	1,260	441	720	79	10	40,000	15,132
12	3 y 2 mo	M	EBV-HLH	5,720	4,347	1,020	83	85	28,410	5,422
13	12 y 6 mo	F	Infection-HLH†	100	70	30	88	34	38,408	6,917

F, Female; *M*, male; *p-HLH*, primary HLH; *RSV*, respiratory syncytial virus.
*Suspected p-HLH, but negative workup for classical cytotoxic pathway gene defects.
†Presumed triggered by RSV.

TABLE E4. Evaluation of HLH-2004 criteria for patients with MIS-C and patients with COVID-19

Laboratory parameters in HLH 2004 criteria	MIS-C*	Percentage†	COVID-19*	Percentage†
Fibrinogen ≤1.5 g/L	1 (57)	1.8	0 (15)	0
Platelets $<100 \times 10^9$/L	10 (60)	16.7	0 (18)	0
ANC $<1.0 \times 10^9$/L	2 (59)	3.4	0 (19)	0
Hemoglobin <90 g/L	2 (60)	3.3	0 (18)	0
Ferritin ≥500 ng/mL	41 (67)	61.2	3 (16)	18.8
sIL-2R ≥2400 U/mL	40 (48)	83.3	7 (21)	33.3

*The number of subjects who had abnormal lab parameters, and the values in parentheses represent the total number of subjects for whom the data were available.
†Percentage of subjects who had abnormal lab parameters as defined in HLH 2004 criteria.